Mini-Review

Discovery of a New Biomotor with a Motion Mechanism Similar to the Earth Revolving around the Sun

Peixuan Guo, Chad Schwartz, Jeannie Haak, and Zhengyi Zhao*

Nanobiotechnology Center, and Markey Cancer Center, Department of Pharmaceutical Sciences, College of Pharmacy, University of Kentucky, Lexington, KY 40536, USA

KEYWORDS: Bionanomotor, AAA+ ATPase Superfamily, One-way Traffic Mechanism, DNA packaging, Virus Assembly, Bionanotechnology.

*Address correspondence to:
Peixuan Guo, Ph. D.
William Farish Endowed Chair in Nanobiotechnology
School of Pharmacy, University of Kentucky
565 Biopharmaceutical Complex
789 S. Limestone Street
Lexington, KY 40536
Email: peixuan.guo@uky.edu
Phone: (859) 218-0128 (office); (513) 728-1411 (cell)

Abstract

Biological nanomotors have previously been classified into two categories: linear and rotational motors. For 35 years, it has been popularly believed that the DNA packaging motors of dsDNA viruses are rotation motors. Recently, a third class of "Revolution Motor" was discovered (see animations http://nanobio.uky.edu/movie.html). By analogy, the Earth revolves 365 days a year around the sun, yet rotates one circle per day upon its own axis. It has been confirmed that the bacteriophage phi29 DNA packaging motor is a hexamer that utilizes a mechanism of revolution instead of rotation. The action by revolution enables a motor free of friction, coiling, and torque; enlightening the mystery of how this small and simple virus can possess such a strong biomotor. This finding has solved many puzzles and debates that have occurred throughout the history of motor studies and settles the discrepancy concerning structure, stoichiometry, and function of DNA translocation motors. This review will also address the puzzles concerning how the motor controls one-way traffic of dsDNA; how the four electropositive lysine layers interact with the phosphate background to generate four steps of pausing during dsDNA translocation; how the motor resolves the mismatch between 10.5 bases and 12 connector subunits per cycle of revolution; how the motor transports closed circular dsDNA without breaking covalent-bonds or changing dsDNA topology; how the motor continues to move without interruption; and why, in certain cases, the motor displays physical motion without the hydrolysis of ATP.

Introduction

The importance of nanomotors for cells or nanotechnology is akin to that of mechanical motors to daily life. Mechanical motors power cars to drive us to destinations; nanobiomotors translocate DNA and RNA to facilitate biological functions. Extensive studies on nanobiomotors have resulted in many fabulous and marvelous findings, but also much wonderment and conjecture, as well as puzzles and mystery; even zealous and fervent debates and disputes. Historically, nanobiomotors have been found to use two types of motor mechanisms: linear motion and rotational motion (Grigoriev, Moll et al., 2004;Vale, 1993).

In the living organism, a common fundamental process is manifested in the process of dsDNA transportation from one cellular compartment to another. The AAA+ superfamily is a class of nanomotors that facilitate a wide range of functions (Zhang & Wigley, 2008;Snider & Houry, 2008;Snider, Thibault et al., 2008;Ammelburg, Frickey et al., 2006); many of which are involved in dsDNA riding, tracking, packaging, and translocation and are critical to DNA repair, replication, recombination, chromosome segregation, DNA/RNA transportation, membrane sorting, cellular reorganization, and many other processes (Martin, Baker et al., 2005;Ammelburg, Frickey et al., 2006). One attraction of these nanomotors is the hexameric arrangements that members of this family often display (Mueller-Cajar, Stotz et al., 2011;Wang, Mei et al., 2011;Aker, Hesselink et al., 2007;Willows, Hansson et al., 2004;Chen, Yu et al., 2002). Despite their functional diversity, the common characteristic of this family is their ability to convert energy obtained from the binding or hydrolysis of the γ-phosphate bond of ATP into a mechanical force, usually involving a conformational change of the ATPase protein. This change of conformation generates both a gain or a loss of affinity for its substrate and a mechanical movement, which in turn is used to either make or break contacts between macromolecules, resulting in local or global protein unfolding, complex assembly or disassembly, or the translocation of DNA, RNA, proteins, or other macromolecules (McNally, Bowman et al., 2010;Guenther, Onrust et al., 1997). The hexagonal shape of the motor facilitates bottom-up assembly in nanomachine manufacturing and produces stable structures, arrangements, and robust machines that may be functionalized in human cells to remedy functional defects.

DsDNA viruses translocate their genomic DNA into preformed protein shells, termed procapsids, during replication (see reviews (Guo & Lee, 2007;Rao & Feiss, 2008;Zhang, Schwartz et al., 2012;Serwer, 2010)). This entropically unfavorable process is accomplished by a nanomotor that uses ATP as an energy source (Guo, Peterson et al., 1987b;Chemla, Aathavan et al., 2005;Hwang, Catalano et al., 1996;Sabanayagam, Oram et al., 2007). The dsDNA packaging motor consists of a protein channel and two packaging molecules to carry out its activities. Our discovery 25 years ago has shown that the larger molecule serves as part of the ATPase complex, and that the smaller one is responsible for dsDNA binding and cleaving (Guo, Peterson et al., 1987b;Guo, Zhang et al., 1998); this notion has now become a well-established definition. Besides the well-characterized connector channel core, the motor of bacterial virus phi29 involves an ATPase protein gp16 (Guo, Peterson et al., 1987b;Guo, Peterson et al., 1987a;Huang & Guo, 2003a;Huang & Guo, 2003b;Lee & Guo, 2006;Lee, Zhang et al., 2008;Ibarra, Valpuesta et al., 2001;Grimes & Anderson, 1990) and a hexameric packaging RNA ring (Guo, Erickson et al., 1987;Guo, Zhang et al., 1998;Shu, Zhang et al., 2007;Zhang, Endrizzi et al., 2012). The motor connector contains a center channel encircled by 12 copies of the protein gp10 that serves as a pathway for dsDNA translocation (Jimenez, Santisteban et al., 1986;Guasch, Pous et al., 2002).

The cellular components that show a strong similarity to viral DNA packaging motor is the FtsK ATPase, an AAA+ motor protein that transports DNA and separates intertwined chromosomes during cell division (Iyer, Makarova et al., 2004); and the SpoIIIE family (Demarre, Galli et al., 2013), an AAA+ protein responsible for the transportation of DNA from mother cell to pre-spore during

Bacillus subtilis cell division (Bath, Wu et al., 2000). The FtsK or SpoIIE DNA transportation systems rely on the assemblage of a hexameric machine. FtsK contains three components: one for DNA translocation, one for the control of orientation, and one for anchoring itself to the substrate (Demarre, Galli et al., 2013). Extensive studies suggest that FtsK may employ a "rotary inchworm" mechanism to transport DNA (Massey, Mercogliano et al., 2006). The FtsK motor encircles dsDNA as a hexameric ring acts in a concerted manner. During each cycle of ATP binding and hydrolysis within each FtsK subunit, one motif acts to tightly bind to the helix while the other progresses forward along the dsDNA. This process causes translational movement and is repeated by the subsequent handing off of the helix to the next adjacent subunit (Massey, Mercogliano et al., 2006). Many other hexameric dsDNA tracking motors function in a similar fashion, including TrwB that is used in DNA transport during bacterial conjugation (Gomis-Ruth, Moncalian et al., 2001); Rad54, an ATPase that supports viral DNA replication (Amitani, Baskin et al., 2006); and RuvB that plays a role in the resolution of the Holliday junction during homologous recombination (Chen, Yu et al., 2002).

Many intriguing packaging models have been proposed for the motor of dsDNA viruses (Serwer, 2010;Maluf, Gaussier et al., 2006;Yu, Moffitt et al., 2010;Moffitt, Chemla et al., 2009;Aathavan, Politzer et al., 2009). For a long time it has been popularly believed that viral DNA packaging motors run through a rotation mechanism that involves a five-fold/six fold mismatch structure (Hendrix, 1978). The most-studied bacteriophage phi29 DNA packaging motor was constructed in 1986 (Guo, Grimes et al., 1986) and also contains three co-axial rings (Fig. 1) (Guo, Peterson et al., 1987b;Lee & Guo, 2006;Ibarra, Valpuesta et al., 2001). In 1987, an RNA component was discovered on the packaging motor (Guo, Erickson et al., 1987); subsequently, in 1998, the RNA particle was determined to exist as a hexameric ring (Guo, Zhang et al., 1998;Zhang, Lemieux et al., 1998) (featured by Cell (Hendrix, 1998)). Based on this structure, in 1998 it was proposed that the mechanism of the phi29 viral DNA packaging motor is similar to that used by other hexameric DNA tracking motors of the AAA+ family (Guo, Zhang et al., 1998). This notion has caused a fervent debate concerning whether the RNA and ATPase of the motor exist as hexamers or as pentamers. Many laboratories have continued to support the pentameric model (Chistol, Liu et al., 2012b;Yu, Moffitt et al., 2010;Morais, Koti et al., 2008) despite the solid finding of the presence of hexameric folds in the motor, as revealed by biochemical analysis (Guo, Zhang et al., 1998;Zhang, Lemieux et al., 1998;Hendrix, 1998;Bourassa & Major, 2002); single molecule photobleaching (Shu, Zhang et al., 2007); gold labelling imaged by electron microscopy (EM) (Xiao, Zhang et al., 2008;Moll & Guo, 2007;Shu, Zhang et al., 2007;Ibarra B, Caston J.R. et al., 2000); nano-fabrication (Xiao, Demeler et al., 2010); and RNA crystal structure (Zhang, Endrizzi et al., 2012). Those who maintain that a pentameric arrangement exists have proposed alternatives to reconcile the pentamer and hexamer debate. One theory states that a hexamer is first assembled on the motor, after which one of the subunits leaves, resulting in the final pentameric state (Morais, Tao Y et al., 2001;Simpson, Tao et al., 2000;Morais, Koti et al., 2008). This proposition has be disputed with findings that motor intermediates isolated during the active DNA packaging process also contain a hexamer (Shu, Zhang et al., 2007). Due to the discrepancy in their data, another group has proposed a further speculation in which one of the subunits in the pentamer ring is inactive and only four of the pentamer subunits rotate during the DNA packaging process (Moffitt, Chemla et al., 2009;Yu, Moffitt et al., 2010).

Many mysteries have been encountered during the course of study of the dsDNA translocation motor. It has been found that the motor transports closed circular dsDNA without breaking any covalent-bonds or changing the DNA topology; that the motor is a one-way traffic machine that controls DNA movement, despite the intrinsic symmetrical nature of the double-stranded DNA helix; and that dsDNA can cross cell membranes without affecting the hydrophobic or hydrophilic nature of the membrane. If the motor were a rotation machine, at least one of the motor components would need to rotate during dsDNA movement; however, extensive studies have revealed that neither the channel

nor the dsDNA rotate during transportation. Four-fold, five-fold, and six–fold models have been proposed or observed for the motor structure and motor mechanism. The above conjectures have been proven by our detection of a novel revolution instead of rotation mechanism. Recently, the phi29 DNA packaging motor has been found to exercise a revolution motion instead of a rotational mechanism (for animation see http://nanobio.uky.edu/movie.html).

In this Mini-Review we focus on addressing the following nine puzzles which, until now, have remained unsolved: 1. *Is the motor a hexamer or a pentamer?* 2. *How can the motor transport the helices without involving rotation, coiling, or a torsion force?* 3. *How does the motor execute the task of one-way traffic directional transportation?* 4. *How do the positively charged lysine layers play a role in the advancement of dsDNA, and how does their interaction with a single strand of the dsDNA phosphate backbone result in four steps of pausing during dsDNA translocation?* 5. *How does the motor resolve the mismatch between one dsDNA helix of 10.5 bases/360° and the connector channel wall comprised of 12 subunits/360°?* 6. How *does the motor transport closed circular dsDNA without breaking covalent-bonds or changing the topology of the DNA?* 7. *How can the motor generate such a strong force?* 8. *How can the motor continue to move without interruption?* 9. *Why, in certain cases, does the motor display physical motion without the hydrolysis of ATP?*

Puzzle 1*: Is the motor a hexamer or a pentamer?*

Besides the sequence homology between phi29 ATPase and other known hexamers, several biochemical assays that have been performed confirm the hexameric arrangement (Schwartz, De Donatis et al., 2013a). Using ATPase fused with green fluorescent protein (GFP), six distinct fluorescent bands were found on native PAGE gel indicative of six monomers oligomerizing to form a hexameric quaternary complex (Fig. 2A). The monomer and all even numbered bands had a higher intensity than the trimer and pentamer, suggesting that the assembling sequence is monomer to dimer to tetramer, and finally to hexamer (Sim, Ozgur et al., 2008;Skordalakes & Berger, 2006;Ziegelin, Niedenzu et al., 2003). As the concentration of gp16 was increased the intensity of the hexamer band also increased significantly, while the intensity of smaller oligomers remained fairly constant. This also suggests that a hexamer is the final oligomeric state.

The presence of eGFP-gp16 hexamer was further confirmed by analytical ultracentrifugation in the presence of a small, 21-nt DNA fragment (data not shown). The resulting species agreed with native gel (Fig. 2A) and electrophoretic mobility shift assay data (EMSA) (Fig. 2B); and were of corresponding sizes indicative of monomers, dimers, tetramers, and hexamers. The formation of gp16 as an active hexameric complex in phi29 DNA packaging was further demonstrated using a Walker B mutant gp16 that could bind, but not hydrolyze ATP; and was analyzed by binomial distribution (Trottier & Guo, 1997;Chen, Trottier et al., 1997). eGFP-gp16 mutated at the Walker B motif (amino acid residues D118 and E119 mutated to E and D, respectively) was found to be completely inactive in DNA packaging. The mutant was mixed with wild-type eGFP-gp16 in different ratios ranging from 10% to 90%, and the activity of the complex was assayed using an *in vitro* viral assembly system (Fig. 4) (Lee & Guo, 1994). The dominant inhibitory activity of the Walker B mutant allowed an independent means of determining the stoichiometry of the ATPase (Trottier & Guo, 1997). The empirical data nearly perfectly overlapped in slope and shape with a theoretical curve representative of a stoichiometry of 6, confirming that the motor complex is hexameric (Fig. 4A). Quantitative and qualitative DNA binding assays were also performed with short, fluorescent dsDNA and eGFP-gp16. Capillary electrophoresis (CE) (Fig. 2A, bottom) and EMSA (Fig. 2B) were employed and it was determined that gp16 binds to the short dsDNA at a ratio of 6:1, further validating our findings that the final oligomeric state of ATPase is hexameric.

Puzzle 2: ***How can the motor transport the helixes without rotating, coiling, or a torsion force?***

This is because the motor exercises a mechanism of dsDNA revolution (see nanobio.uky.edu/file/motion.avi) that has only be recently revealed as a unidirectional movement (Mi, Liu et al., 2010) by way of a "push through a one-way valve" mechanism (Schwartz, Fang et al., 2012;Fang, Jing et al., 2012) that agrees nicely with the previously proposed ratchet (Serwer, 2003) and compression (Ray, Sabanayagam et al., 2010;Ray, Ma et al., 2010) models. Data leads to the conclusion that the hexameric stoichiometry and the mechanism of revolution for phi29 DNA packaging motor are in accordance with FtsK of the hexameric AAA+ superfamily; it is expected that most phages follow the "push through a one-way valve" via revolution mechanism (Zhao, Khisamutdinov et al., 2013a;Schwartz, Zhang et al., 2013b). The "push through a one-way valve" mechanism describes dsDNA as being pushed through the connector channel by the ATPase gp16 in an entropically unfavorable process while the connector functions like a valve to prevent DNA from slipping out of the capsid during the packaging process (Black, 1989;Feiss & Rao, 2012;Casjens, 2011;Guo & Lee, 2007); a feat that is accomplished by a DNA-packaging motor that uses ATP as an energy source.

It has been found that the phi29 motor contains six copies of the ATPase gp16, as discussed in the previous section. The binding of ATP to one subunit stimulates ATPase to adapt to a conformation with lower entropy, but a higher affinity for dsDNA. Upon ATP hydrolysis, the ATPase assumes a new conformation with high entropy and a lower affinity for dsDNA, thus pushing dsDNA away from the subunit and transferring it to an adjacent subunit by a power stroke. The cooperativity and sequential action among hexameric ATPase subunits (Chen & Guo, 1997a;Moffitt, Chemla et al., 2009), as determined by Hill constant and binomial distribution assays of the inhibition performed by mutant subunits (Fig. 4), also promotes the revolution of dsDNA along the connector channel. The contact between the connector and the dsDNA chain is transferred from one point on the phosphate backbone to another point along a single strand in a 5' to 3' direction; also demonstrated in another report (Moffitt, Chemla et al., 2009). The DNA revolves unidirectionally along the hexameric channel wall, but neither the dsDNA nor the hexameric ring rotates. One ATP is hydrolyzed in each transitional step and six ATPs are consumed in one cycle to translocate the dsDNA one helical turn of 360°. The binding of ATPase on the channel wall along the same phosphate backbone chain, but at a location 60° different from the last contact, urges dsDNA to move forward 1.8 bp each step (10.5 bp per turn ÷ 6 ATP = 1.8 bp/ATP) and revolve; thus, the rotation of neither the hexameric ATPase ring nor the dsDNA is required for DNA translocation.

Specifically, the helices revolve without rotating, coiling, or a torsion force because of the anti-parallel arrangement between the dsDNA helix and the channel subunits of both the connector dodecamer and the ATPase hexamer, as revealed by crystallography (Fig. 1) (Guasch, Pous et al., 2002;Simpson, Leiman et al., 2001). The connector helix has 12 subunits that each displays a tilt of 30°. When one helix of dsDNA advances 360°, the dsDNA shifts 30° every time it passes one of the 12 subunits (360° ÷ 12 = 30°) (Fig. 1 & 5). The term "anti-parallel" means to twist with opposite orientation, and refers to each step of the advancing DNA where the DNA changes +30° and the angle is compensated for by the -30° tilting of the subunit of channel wall. The "+" and the "-" occur because of the anti-parallel arrangement. A "+30°" displacement interact with a "-30^{0}" displacement and results in a net value of "0"— the reason why the motor transports the helixes without involving rotation, coiling, or a torsion force.

Puzzle 3: ***How does the motor execute the task of one-way traffic directional transportation?***

It has been demonstrated that the motor uses a "push through one-way valve" mechanism to translocate dsDNA (Jing, Haque et al., 2010;Zhang, Schwartz et al., 2012); as verified by voltage ramping, electrode polarity switching (Fig. 6C), and sucrose sedimentation assessment (Jing, Haque et al., 2010). The direction of translocation is controlled by five actions: 1) the motor ATPase undergoes a series of entropy transitions and conformational changes during the binding of ATP and dsDNA. The hydrolysis of ATP results in a second change in entropy and conformation of the ATPase, one with a low affinity for dsDNA that causes it to push the dsDNA to advance and revolve within the channel; 2) the 30° tilting angle of each subunit of the dodecameric connector channel that runs anti-parallel to the dsDNA helix facilitates the one-way traffic of the dsDNA and coincides with the 12 subunits of the connector channel (360° ÷ 12 = 30°) that serve to enhance the translocation of dsDNA in a single direction, as revealed by crystallography; 3) the unidirectional flowing property of the internal channel loops serves as a ratchet valve to prevent dsDNA reversal; 4) the 5'-3' single-direction revolving translocational movement of one strand of dsDNA along the phi29 motor connector channel wall ensures a unidirectional motion; and 5) four lysine layers interacting with a single strand of the dsDNA phosphate backbone, resulting in four steps of transition and pause during dsDNA translocation.

DsDNA runs through the connector, potentially making contact at each subunit (Fig. 1). The anti-parallelism exhibited by the helices argues against a bolt and screw rotation model, since a screw thread and the corresponding whorl should display parallel transport. We constructed a mutant connector in which the internal loop containing residues 229-246 was deleted. Procapsids with a loop-deleted connector fail to produce any virions (Fig. 6B). The packaged dsDNA reverses direction and slides out of the mutant procapsid after being packaged (Fang, Jing et al., 2012;Geng, Fang et al., 2011;Grimes, Ma et al., 2011;Serwer, 2010;Isidro, Henriques et al., 2004). The channel loops may act as a ratchet, though, during DNA translocation to prevent the DNA from leaving, supporting the "push through one-way valve" model (Fig. 6A) (Fang, Jing et al., 2012). When all of the internal loops are deleted, translocation of dsDNA through the connector is blocked, as demonstrated by single pore conductance assay (Fang, Jing et al., 2012), the one way traffic channel becomes a two-way traffic channel for ssRNA or ssDNA (Fig. 6D) (Geng, Fang et al., 2013). Thus, the connector is a one-way valve (Lee & Guo, 1994;Hendrix, 1978;Hugel, Michaelis et al., 2007) that only allows dsDNA to move into the procapsid unidirectionally (Wendell, Jing et al., 2009).

In-depth investigations into data, modeling, and literature have led to the following conclusion: the motor only uses one strand of the dsDNA, not both, packages in the 5'→3' direction, interacts with a lysine ring, and revolves along the channel (Lee & Guo, 1995;Lee & Guo, 1994). It has been found that phi29 DNA with single-stranded gaps is not packaged at full genome length, though. Hence, another experiment was conducted where two gaps were created in the phi29 DNA genome: one at the left end and one at the right end. Only a 5.9 kb DNA fragment between the left end of the genome and the first gap were packaged (Moll & Guo, 2005), but the right end fragment was not. The results suggest that a single-stranded gap in DNA can cause the packaging motor to stop; and that the packaging direction is from the 5'c3' end. This model is further supported by the finding by Black and co-workers (Oram, Sabanayagam et al., 2008) that a 3' end extension up to 12 bases does not inhibit translocation, and 20 or more bases significantly block the T4 motor in DNA packaging. These results support the notion that the motor can revolve one complete turn of 360° with a single-stranded structure, and that dsDNA revolves along the motor using a single strand that is packaged in the 5's3' direction. The data is also supported by the findings that dsDNA is processed by having contact with an unknown component on one strand of DNA in the 5'd by tweezer, and that modified phi29 DNA stops dsDNA packaging; as revealed by optical tweezers. Modification of 10 bases has been found to be tolerable, but the changing 11 bases is not (Aathavan, Politzer et al., 2009). The evidence reveals that the four distinct motor steps occur because of the alternating positive and negative charges on the connector channel wall, a

condition which alters the speed of DNA translocation and results in four steps of pausing during advancement— all due to the mechanism of revolution.

Puzzle 4: ***How do the positively charged lysine layers play a role in the advancement of dsDNA; and how does their interaction with a single strand of the dsDNA phosphate backbone result in four steps of pausing during dsDNA translocation?***

Connector crystal analysis (Guasch, Pous et al., 2002) has revealed that the negatively charged phi29 connector interior channel surface is decorated with 48 positively charged lysine residues. The residues exist as four 12-lysine rings and are derived from the 12 protein subunits that enclose the channel (Fig. 7 & 8). In the past, the four lysine rings (K200, K209, K234, and K235) scattered inside the channel have been proposed to play a role in DNA translocation (Guasch, Pous et al., 2002). However, it has been found that mutation of one of the layers of the four lysine rings does not significantly affect motor action (Fang, Jing et al., 2012). Further investigation of the detailed interaction of the lysine residues with the bacteriophage genome during translocation suggests that that when DNA revolves through the connector, it goes through 12 subunits of the connector per cycle, with only one strand touching the channel wall. Thus, during the entire 360° revolution, it is proposed that the negatively charged phosphate backbone makes contact with the same positively charged layer of the lysine ring (Schwartz, De Donatis et al., 2013b;Schwartz, Zhang et al., 2013a;Zhao, Khisamutdinov et al., 2013b).

The crystal structure shows that the length of the connector channel is 7 nm (Guasch, Pous et al., 2002;Jimenez, Santisteban et al., 1986;Badasso, Leiman et al., 2000). Vertically, four lysine layers fall within a 3.7 nm (Guasch, Pous et al., 2002) range and are spaced approximately ~0.9 nm apart (Fig. 7 & 8). Since B-type dsDNA has a pitch of 0.34 nm/bp, ~2.6 bp exist per rise along its axis that interact with dsDNA ($0.9\ \mathrm{nm}/0.34\ \mathrm{nm.\,bp^{-1}} = \sim 2.6\ \mathrm{bp}$). During the entire 360° revolution, the negatively charged phosphate backbone of dsDNA makes contact with the same positively charged lysine layer located inside the channel. For every 10.5 bp of B-type dsDNA, it is suggested that one strand of DNA revolves 360° through the channel, resulting in a mismatch ($10.5 \div 12 = 0.875$) between the base with the negatively charged phosphate group and the channel subunits with positively charged lysine ring. On average, each of the four lysine layers are responsible for contact with three subunits (12 subunits ÷ 4 layers = 3 subunits). This value indicates that for every three subunits, 2.6 bp will be translocated through the connector ($0.875 \times 3 = 2.6\ \mathrm{bp}$).

It is proposed that the dsDNA phosphate backbone interacts with the optimally charged lysine in the next subunit, and the distance variation due to this mismatch is compensated for by the introduction of the next lysine layer (Fig. 7 & 9) (see **Puzzle 5**). The four layers of the lysine ring will result in four pauses of DNA translocation. This is in agreement with the finding that four steps of transition and pausing were observed during translocation, and that each pause per step corresponds to the translation of 2.5 base pair of phi29 dsDNA; although others have interpreted that the pausing is due to an inactive subunit of the five-subunit structure of the motor (Chistol, Liu et al., 2012a;Moffitt, Chemla et al., 2009).

Puzzle 5: ***How does the motor resolve the mismatch between one dsDNA helix of 10.5 bases/360° and the connector channel wall comprised 12 subunits?***

As indicated above, data indicates that during the entire 360° revolution the negatively charged phosphate backbone of dsDNA makes contact with the same positively charged lysine layer located inside the channel. For every 10.5 bp of B-type dsDNA, one strand of DNA revolves 360° through the 12-subunit channel, resulting in a mismatch ($10.5 \div 12 = 0.875$) between the base with negatively a

charged phosphate group and the channel subunits with a positively charged lysine ring. At each step of dsDNA translocation, a 12.5% mis-match (1 - 0.875 = 0.125) occurs between the dsDNA helix and the connector channel wall. The distance variation due to this mismatch is compensated for by the introduction of the next lysine layer (Fig. 7C & 9). Since the 12-subunit channel has four layers, , each lysine layer is responsible for contact with an average of three subunits (12 subunits ÷ 4 layers = 3 subunits). After three transactions, a 37.5% mismatch occurs (12.5% × 3 =37.5%). The distance variation due to this mismatch is compensated for by the introduction of the next lysine layer (Fig. 7C & 9), and the contact point between the phosphate and the lysine shifts to a spot on the next lysine ring where the phosphate can make its next contact. This transition results in a slight pause in DNA advancement. When dsDNA translocates through three subunits, the leading phosphate transitions into the next lysine layer in order to compensate for the imperfect match that occurs between the phosphate and each lysine residue, during DNA advancement through the connector (Fig. 7C & 9).

It has been found that the mutation of only one layer of the four lysine rings does not significantly affect motor action (Fang, Jing et al., 2012), indicating that the interaction of lysine and phosphate is only an auxiliary force, but not the main force involved in motor action. This also indicates that the uneven speed of the four steps of transition and pausing caused by the four lysine layers is not an essential function of the motor. This explains why the lysine layers and the 10.5 bases per helical turn are not a perfect match, and why the distance between layers is not constant.

Puzzle 6: ***How does the motor transport closed circular dsDNA without breaking any covalent-bonds or changing the topology of the DNA?***

The ATPase monomer (not the hexamer) binds to dsDNA. After ATP binding, the ATPase subunit decreases in entropy and changes conformation, leading to a high affinity for dsDNA and the ability assemble as a hexamer on DNA without the requirement of ATP hydrolysis. Therefore, the motor assembles into a hexamer on the DNA itself, rather than the insertion of the dsDNA molecule into a preformed hexamer. A free 5′ or 3′ dsDNA end is not required, and the motor can theoretically transport closed circular dsDNA without breaking covalent bonds or changing DNA topology.

It is commonly believed that the binding of ATPase gp16 to the viral procapsid to form a complex is the first step in motor function during DNA packaging (Fujisawa, Shibata et al., 1991;Guo, Peterson et al., 1987a). However, it has been found that the first step in phi29 DNA packaging is instead the binding of multiple gp16 in a queue along the dsDNA (Fig. 10B). A string of multiple Cy3-gp16 complexes have been observed on dsDNA chains that have been lifted by, and stretched between, two polylysine-coated silica beads in the presence of non-hydrolyzable γ-S-ATP (Fig. 10B). This suggests that the queuing of ATPase gp16 along the DNA is the initial step in phi29 DNA packaging. Upon a conformational change stimulated by ATP binding, single subunits gather around the dsDNA chain first and then form a complex surrounding the DNA. It has been noted that both ends of the dsDNA were tethered to the beads, an observation which proves that a free 5′ or 3′ dsDNA end is not required for the ATPase to bind dsDNA, and that assembly of the hexameric gp16 ring occurs only upon binding to DNA (Fig. 10C). Negatively stained electron microscopy images provides additional evidence of multiple gp16 complexes occurring along phi29 genomic DNA (Fig. 10B), lending further support to the conclusion.

Puzzle 7: ***How can the motor generate such a strong force?***

The phi29 packaging motor is one of the strongest biomotors constructed to date, providing forces up to 57 pN (Smith, Tans et al., 2001). It has recently been found that five different forces are involved in packaging DNA into a preformed shell during viral maturation, and all are needed to

generate such a large force. Data indicates that the first force occurs when the binding of ATP to gp16 promotes a favorable entropic change in gp16, leading to a conformational change with an associated 40-fold enhancement in affinity for dsDNA (Fig. 11). The binding of only one ATP to the hexameric gp16 is sufficient to induce strong DNA-binding (Fig. 12). The second force is a result of ATP hydrolysis by a DNA-bound subunit of the hexamer that induces a second conformational and entropic change, resulting in a low affinity state for dsDNA; a step that enables the subunit to push dsDNA forward to the next subunit of the ATPase. It is proposed that the third force is created because of the unique 30° tilt of the connector subunits relative to the vertical axis of the channel. When dsDNA binds to each of the 12 subunits in succession, the anti-parallel arrangement between two helices of the connector subunit and dsDNA produces potential energy for the dsDNA helix to revolve in a single direction, with a 30° transition for each subunit. Thus, the dsDNA migrates a complete helical turn while it revolves through the 12 subunit channel (30° x 12 = 360°). A similar force can be generated from the anti-parallel arrangement between the channel of the ATPase channel and the dsDNA helix. The fourth force involves the revolution, rather than rotation, of the dsDNA around the ATPase ring. Similar to the channel mechanism, the revolution and advancement of one strand of dsDNA generates potential energy to ensure the one-way advancement of dsDNA, without the involvement of a coiling or tension force. It is suggested that the fifth force is produced by the one-way flow loops within the channel that provide a vector force for DNA to enter the capsid, but not to leave it. The motor uses 6 ATP to complete one revolution, and one ATP is needed to package 1.75 bp of dsDNA (10.5 bp ÷ 6 ATP = 1.75 bp/ATP).

Puzzle 8: ***How can the motor continue to move without interruption?***

Hill constant determination and binomial distribution of inhibition assay have led to the conclusion that ATPase subunits work sequentially and cooperatively (Fig. 4). This action enables the motor to work continuously without interruption, although pauses have been observed (see **Puzzle 4, 5**). In a single phrase: cooperativity among motor subunits allows the motor to continue to move without interruption. It has been found that only one ATP-activated subunit in the hexamer is needed to strongly bind dsDNA to the motor hexamer. The amount of DNA bound to gp16 by keeping the concentration of gp16 and DNA constant and varying the concentration of γ-s-ATP in the reaction mixture (Fig. 12). If more than one γ-s-ATP per oligomer of gp16 were required to generate a high affinity state for DNA, the plot would show a cooperativity profile with a Hill coefficient representative of the amount of γ-s-ATP required to be bound to gp16. In principle, a Hill coefficient close to 1 indicates that only one γ-s-ATP-activated subunit in the oligomer is required for DNA binding, or that the binding of DNA is progressively increased with the number of subunits that are bound to γ-s-ATP. Data from the study exhibited no cooperativity in binding and a Hill coefficient of 1.5, indicating that all of the subunits of gp16 do not need to be bound to γ-s-ATP in order to stabilize DNA binding.

An experiment was performed in manner similar to the CE assay described above. The complex of gp16-DNA was assembled in the presence of saturating conditions of γ-s-ATP and after formation of the complex, increasing amounts of ADP were added in order to compete with γ-s-ATP for the active sites of gp16 and ultimately promote the release of DNA. The results indicated the presence of a remarkably cooperative behavior (Fig. 12). From the resulting fractional inhibition plot a Hill coefficient close to 6 was extrapolated, indicating that six molecules of ADP are required to bind to gp16 before the dsDNA can be released from the protein. This also indicates that only one ATP bound subunit is able to stably bind DNA and prevent ADP-mediated release. Furthermore, results indicate that gp16 most likely binds to dsDNA at only one subunit per round of ATP hydrolysis.

As mentioned above, a Hill coefficient close to 1 indicates that binding of DNA has progressively increased with each number of subunits that are bound to γ-s-ATP. However, the 3.6-nm diameter of the motor channel, as measured from the crystal structure (Guasch, Pous et al., 2002), suggests that only one dsDNA can be bound within the channel. This indicates that dsDNA shifts to a subsequent gp16 subunit upon release of the former. These results, in combination with the finding that one Walker B mutant gp16 is sufficient to block the motor for DNA packaging, support the model that the ATPase motor works sequentially. Upon ATP hydrolysis, the subunit of the ATPase gp16 assumes a new conformation in order to push dsDNA away from a subunit and transfer it to an adjacent subunit (Fig. 10A).

The binding of dsDNA to only one gp16 subunit at a time suggests that gp16 undergoes cooperativity during DNA translocation. To verify this hypothesis, ATPase activity was analyzed by studying the effects of introduced mutant subunits on the oligomerization of gp16 (Trottier & Guo, 1997;Chen, Trottier et al., 1997). If communication between the subunits of the ATPase is assumed, then the effect of the mutation of one inactive subunit on the ATPase activity should be higher than the simple sum of the ATPase activity of a single subunit. Increasing amounts of Walker B mutants added to the overall gp16 oligomer failed to provide any significant effect on the rate of hydrolysis when the ATPase activity was measured in the absence of dsDNA (Fig. 13). This suggests that each subunit of gp16 is able to hydrolyze ATP independently. But, when saturating amounts of dsDNA were added to the reaction, a strong negative cooperative effect was produced with a profile that mostly overlapped with a predicted profile in which one single inactive subunit was able to inactivate the whole oligomer (Fig. 13). This predicted case was calculated from binomial distribution inhibition assay (Trottier & Guo, 1997;Chen, Trottier et al., 1997) and produced results suggesting that, in the presence of dsDNA, a rearrangement occurs within the subunits of gp16 that enable them to communicate with each other and "sense" the nucleotide state of the reciprocal subunit.

Furthermore, the fact that dsDNA needs to be present in the reaction indicates that dsDNA binds to the inactive subunit during the catalytic cycle and remains bound to it, a condition that generates a stalled ATP hydrolysis cycle. Moreover, this observation supports the idea that only the subunit that is bound to the substrate at any given time is permitted to hydrolyze ATP. Thus, translocation is performed while the other subunits are in a type of "stalled" or "loaded" state. The above scenario suggests an extremely high level of coordination in the function of the protein, which is likely the most efficient process of coupling energy production via ATP hydrolysis and DNA translocation. An effective mechanism of coordination is apparent between gp16 and dsDNA using the hydrolysis cycle as means for regulation. The cooperativity and sequential action among hexameric ATPase subunits (Chen & Guo, 1997b;Moffitt, Chemla et al., 2009) promotes the revolution of dsDNA along the channel (Fig. 14). This model suggests that contact between the connector and the dsDNA chain is transferred from one point on the phosphate backbone to another point, which also agrees with previous reports (Moffitt, Chemla et al., 2009).

Puzzle 9: ***Why, in certain cases, does the motor display physical motion without the hydrolysis of ATP?***

The classical dogma follows that nanobiomotors are powered by the energy released from ATP hydrolysis. Although the process of converting the chemical energy stored in ATP to physical motion is still unknown, several reports have indicated that the onset of motion can be linked to ATP binding, rather than ATP hydrolysis (Kinosita, Jr., Yasuda et al., 2000;Chang, Andrews et al., 2012;Acharya, Foster et al., 2003;Gradia, Acharya et al., 1997;Gradia, Subramanian et al., 1999). Similar to AAA+ motor proteins that undergo a cycle of conformational changes between two distinct states during their interaction with ATP, the phi29 motor ATPase gp16 (Guo, Peterson et al., 1987b;Ibarra, Valpuesta et

al., 2001;Lee, Zhang et al., 2008), which provides energy to the motor via ATP hydrolysis, also displays high and low affinity states for DNA substrate. Recently, it has been qualitatively demonstrated via EMSA that gp16 is capable of binding to dsDNA and exhibits stronger binding to DNA in the presence of γ-S-ATP, a non-hydrolysable ATP analog (Schwartz, Fang et al., 2012). This finding has been further validated by Forster Resonance Energy Transfer (FRET) analysis and sucrose gradient sedimentation, which both demonstrate that the gp16/dsDNA complex is stabilized by the non-hydrolyzable ATP substrate. However, a set of questions then arose concerning how motor can promote motion at its first step, without the hydrolysis of ATP, and where does the energy come from?

It is proposed that during motor motion, the major driving force is the entropy transition, not the heat flow. The motor ATPase undergoes a cycle of conformational changes between two distinct states during their interaction with ATP (Guo, Peterson et al., 1987b;Ibarra, Valpuesta et al., 2001;Lee, Zhang et al., 2008). The first step is the ATP binding, which results in the reduction of the entropy in the ATPase by a conformational change. The entropy lost in this step is compensated by a subsequent step of ATP hydrolysis that results in the gaining of entropy with a conformational residue. Thus, the motor ATPase displays high and low affinity states for DNA substrate in response to the binding and hydrolysis of ATP. It was then proposed that ATP binding decreases the entropy in the ATPase, induces a conformational change, and acts as the first force generating step of motor motion— without ATP hydrolysis. The conformational change is a process that couples motion with the transition of entropy as an intrinsic property of the protein. More specifically, we proposed that the classical P-loop of the AAA+ family was directly responsible for ATP binding and the transition of ATPase into a more entropically favorable conformation.

It has also been predicted that the presence of both a DNA binding domain and a Walker-A motif in ATPase gp16 (Schwartz, Fang et al., 2012). In AAA+ proteins, the consensus is that the Walker A motif is responsible for ATP binding, while the Walker B motif initiates ATP hydrolysis (Story & Steitz, 1992). The Walker A motif in the phi29 ATPase gp16 has been identified previously (Guo, Peterson et al., 1987b), and confirmed by mutation assay (Chad Schwartz, Gian Marco De Donatis et al., 2013). The binding of ATP promotes the ATPase gp16 to adapt a high affinity conformation for dsDNA binding. However, this conformational change induced by ATP binding disappears when a mutation is introduced to the Walker A motif (Fig. 15); and the ATPase activity of the Walker A mutant is rendered undetectable due to its inability to bind ATP. To investigate the mechanism further, the gp16/dsDNA/γ-S-ATP complex was purified by sucrose gradient sedimentation and subjected to an ATP hydrolysis kinetic assay (Chad Schwartz, Gian Marco De Donatis et al., 2013). After correlation of the ATP hydrolysis with the release of dsDNA from the gp16, the results suggested that the release of inorganic phosphate from the P-loop spurned ATPase to gain entropy; garnering another shift in conformation that forced the DNA substrate away from the interior pocket of the ATPase; and causing the genomic DNA to physically move towards the capsid. However, this catalytic force step is eliminated when a mutation is introduced to the Walker B motif of gp16 (Fig. 3 & 15), a finding that agrees other reports that report that Walker B mutants do not hydrolyze ATP, but still maintain strong binding to DNA. In summary, after the first force generation via ATP binding, the subsequent ATP hydrolysis promotes the gp16 to undergo a further conformational change; produce an external force against dsDNA; and push the substrate away from the motor complex by a power stroke that causes the next step in motion to occur (Fig. 14).

Concluding Remarks

The stoichiometry of the phi29 DNA packaging motor has long been a subject of debate (Hendrix, 1978;Shu, Zhang et al., 2007;Zhang, Schwartz et al., 2012;Guo, Zhang et al., 1998;Moffitt, Chemla et al., 2009;Yu, Moffitt et al., 2010;Guo, Zhang et al., 1998;Zhang, Lemieux et al.,

1998;Hendrix, 1998;Shu, Zhang et al., 2007;Xiao, Zhang et al., 2008;Moll & Guo, 2007;Shu, Zhang et al., 2007;Xiao, Demeler et al., 2010;Zhang, Endrizzi et al., 2012); nevertheless, both camps believe that the ATPase and pRNA exist in a 1:1 stoichiometric ratio. But, inconsistent stoichiometry has also been reported in other phage systems (Maluf, Gaussier et al., 2006;Roy, Bhardwaj et al., 2011a). Further biochemical data proves that pRNA is capable of forming hexamers, and that the ATPase consists of six subunits in a concentration dependent manner (Fig. 2A), upon binding to dsDNA (Fig. 2B), and on the active phi29 motor (Fig. 4). It has been found that the phi29 DNA packaging motor revolves without rotating, coiling, or generating torque (Schwartz, et al. *Virology* accompanying paper). Since the revolution mechanism is independent of stoichiometry of motors subunits, motors with different stoichiometry subunits all can utilize the revolution mechanism. Therefore, the discovery of the revolution mechanism might reconcile the stoichiometric discrepancy among many phage systems for which ATPase was found to be present as tetramer (Maluf, Gaussier et al., 2006), hexamer (Guo, Zhang et al., 1998;Zhang, Lemieux et al., 1998;Hendrix, 1998;Shu, Zhang et al., 2007;Xiao, Zhang et al., 2008;Moll & Guo, 2007;Shu, Zhang et al., 2007;Xiao, Demeler et al., 2010;Zhang, Endrizzi et al., 2012), or nonamer (Roy, Bhardwaj et al., 2011b).

The discoveries discussed in this review offer a series of applications in nanotechnology. The riding system along one string of dsDNA provides evidence of a motion system for cargo transportation at the nanoscale, and a tool for studying force generation mechanisms in a moving world. The revolution mechanism itself offers a prototype for a new motor involving forward motion, such as that used by roller coasters or trolley cars that can use a helical axis to promote forward motion. The transition of dsDNA along 12 channel subunits offers a series of recognition sites on the dsDNA backbone and provides additional spatial variables for nucleotide sensing in the discrimination of nucleotides based on distance parameters. Nature has evolved a clever machine that translocates the DNA double helix and avoids the difficulties associated with rotation, e.g. DNA supercoiling, that have been observed in many other processes. A video of dsDNA translocation be found at nanobio.uky.edu/file/motion.avi.

Acknowledgements

The work was supported by NIH grants R01 EB003730, R01 EB012135, and U01 CA151648 to PG, who is a co-founder of Kylin Therapeutics, Inc. and Biomotor and Nucleic Acids Nanotech Development, Ltd.

Figures

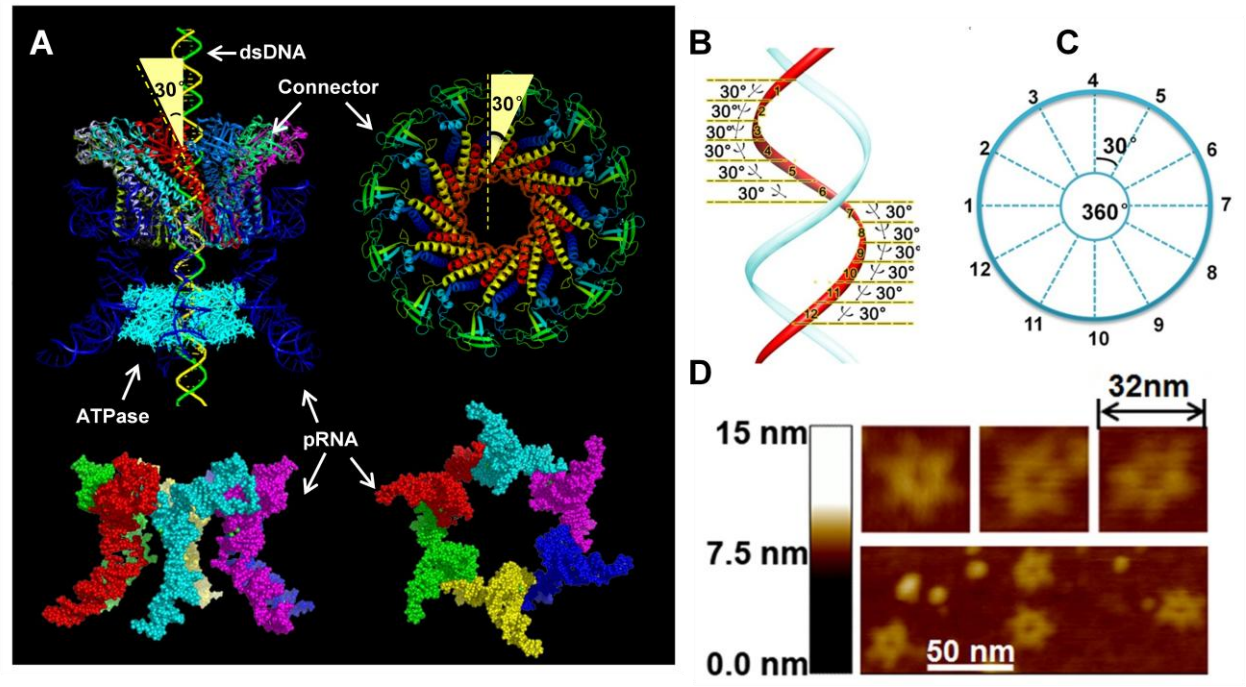

Figure 1. Illustration of the phi29 DNA-packaging motor hexametric structure. **(A)** Side view of the phi29 packaging motor and pRNA hexamer (left bottom), and top view of the phi29 connector (right top) and pRNA hexamer (right bottom). The 30° tilt of the helix of the connector subunit is depicted as an external view and an internal view. **(B)** One twelfth of a dsDNA helix is 30°, which is **(C)** the angle that dsDNA revolves through to advance between two adjacent connector subunits. The contact at every 30° for twelve 30° transitions translocates dsDNA one helical turn through the connector. (**D**) AFM images of modified pRNA hexamer.

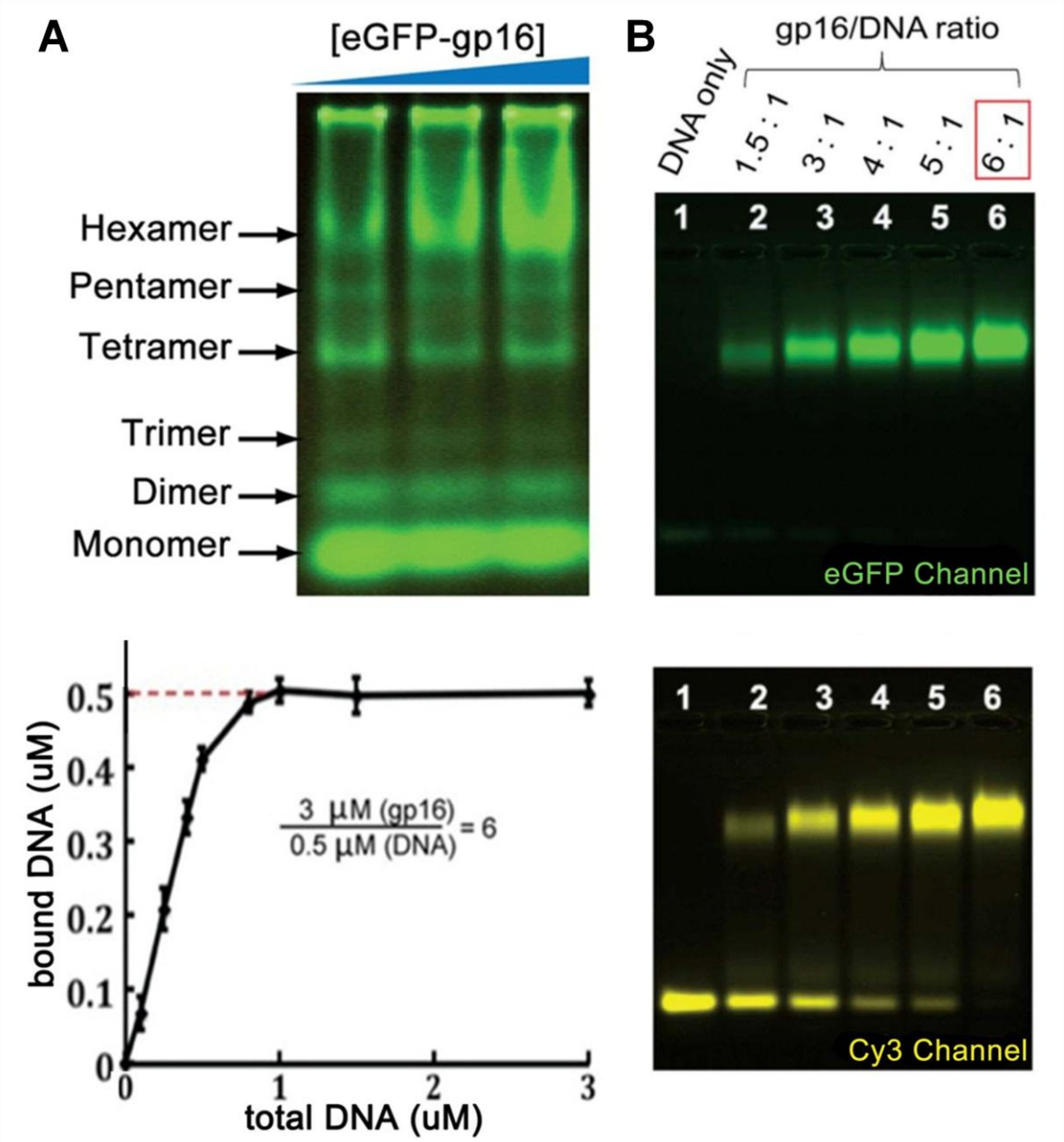

Figure 2. Biochemical stoichiometric assays showing the formation of gp16 hexamer. (A) Native PAGE reveals six distinct bands characteristic of the six oligomeric states (upper) and capillary electrophoresis quantification (lower) by varying the molar ratio of [protein]:[DNA]. The concentration of bound DNA plateaus at a molar ratio of 6:1 as [protein] remained constant. Analytical centrifugation of gp16 plotted as particle size (upper) and sedimentation coefficient (lower), respectively. A Gp16 hexamer was formed and two spots of gp16 appeared that had similar particle size, but different sedimentation coefficients due to particle conformation, indicating that gp16 hexamer has two conformations with and without DNA. Analytical Ultracentrifugation is carried out under 20 kpm, and the data is derived after refining the 2DSA Monte Carlo analysis with a genetic algorithm/Monte Carlo fit. **(B)** Slab gel EMSA of gp16 binding to dsDNA with mutated Walker motifs in a 6:1 ratio; imaged by GFP and cy3 channels for gp16 and dsDNA, respectively.

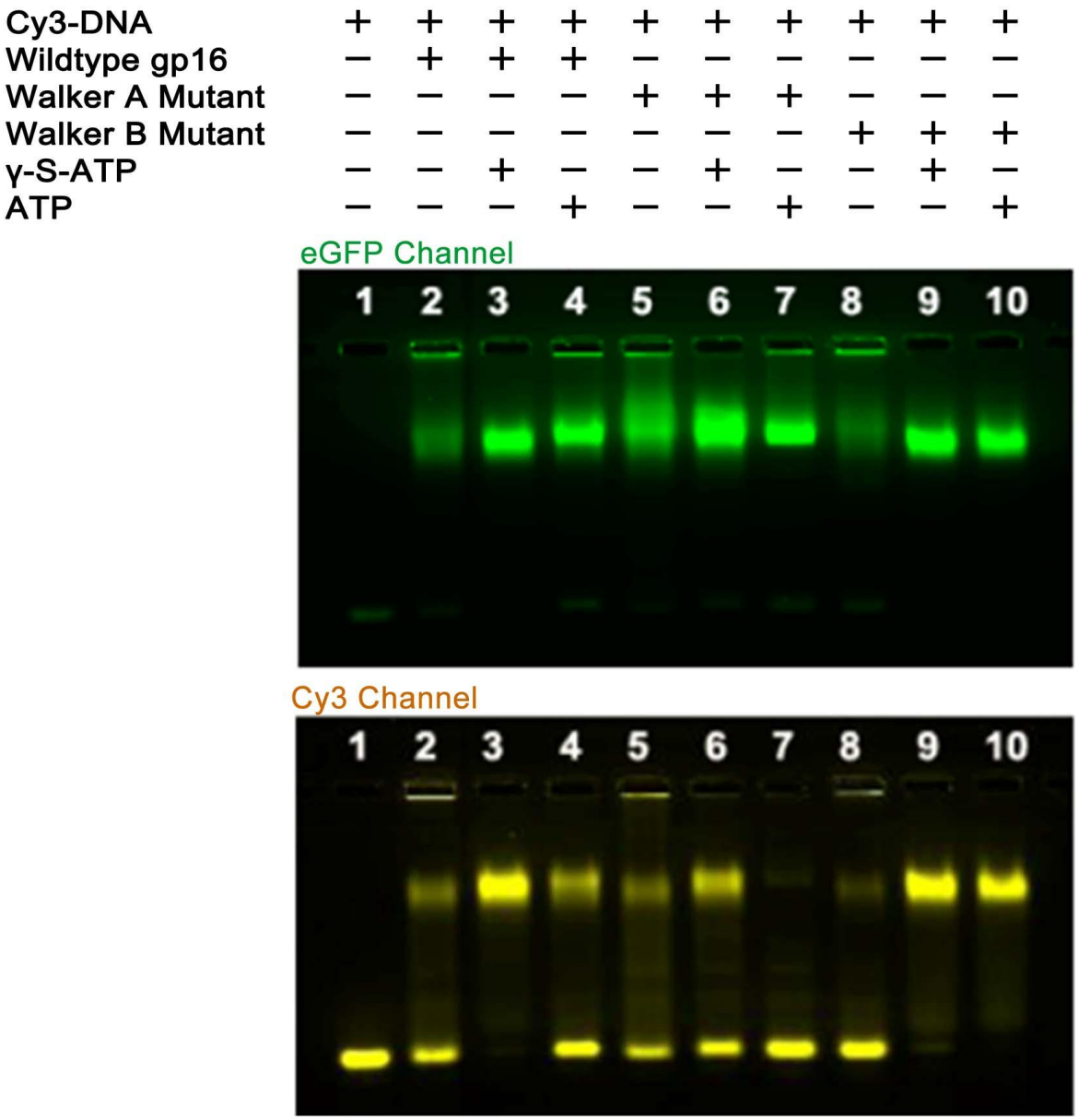

Figure 3. DNA Binding Assays. Slab gel EMSA of gp16 binding to dsDNA with mutated Walker motifs; imaged by GFP and cy3 channels for gp16 and dsDNA, respectively.

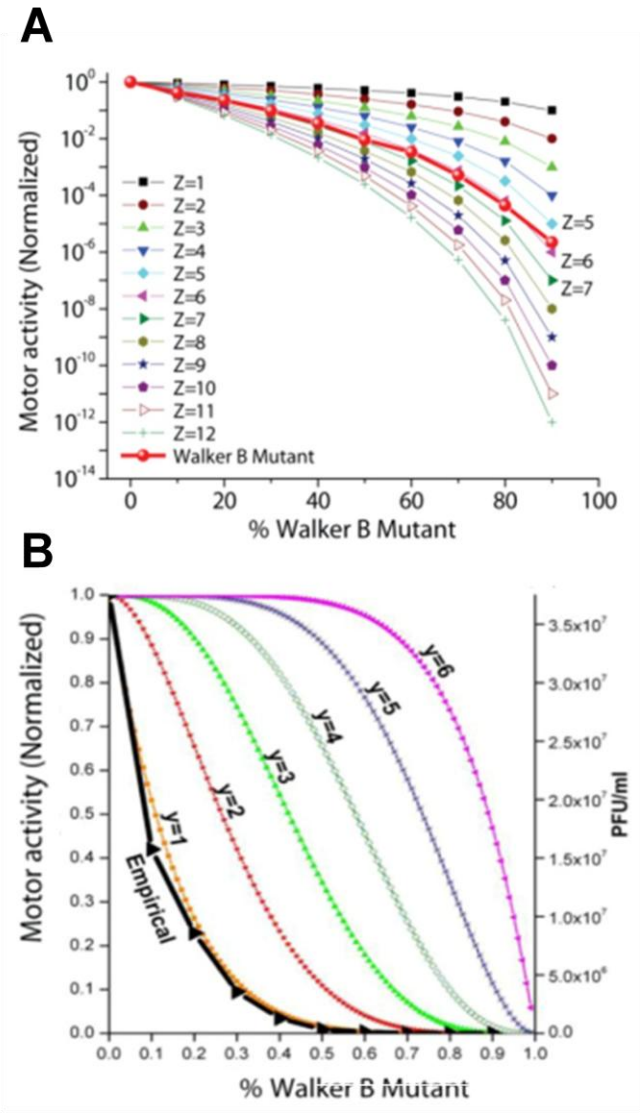

Figure 4. Viral assembly inhibition assay using a Walker B mutated motif by binomial distribution. Binomial distribution revealing that **(A)** gp16 possesses a 6-fold symmetry in the DNA packaging motor, and **(B)** that the mutation of one Walker B subunit within the hexamer blocks motor activity demonstrating cooperativity.

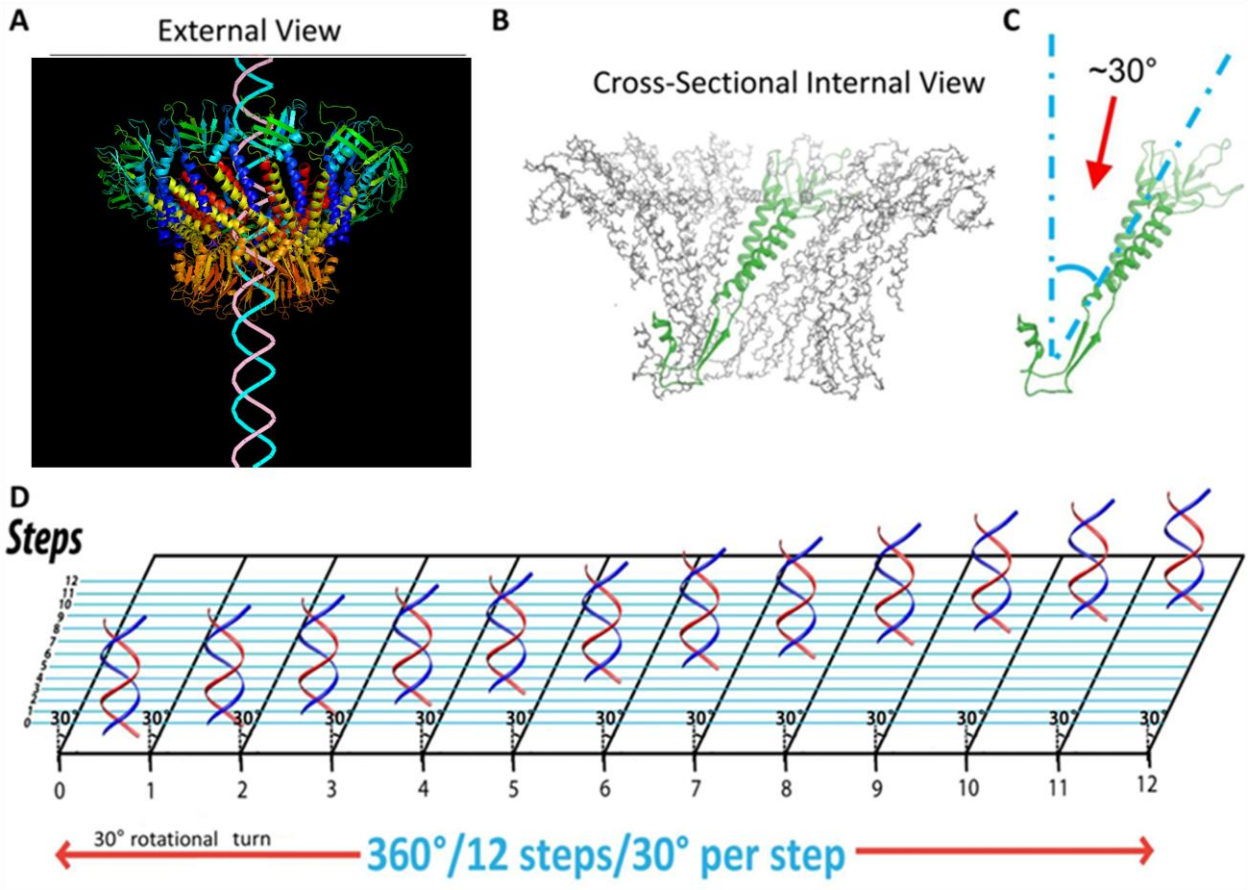

Figure 5. DNA revolves and transports through 30° tilted connector subunits facilitated by the anti-parallel arrangement between dsDNA helixes and connector protein subunits. (A,B) The anti-parallel configuration can be visualized in which DNA revolves through the connector, **(C)** making contacts at every 30° transition. A planar view is suggested **(D)** in which DNA advances and travels along the circular wall of the connector channel with no torsion or coiling force and continues through the connector channel, touching each subunit, translocating 12 discrete steps at 30° integrals per subunit.

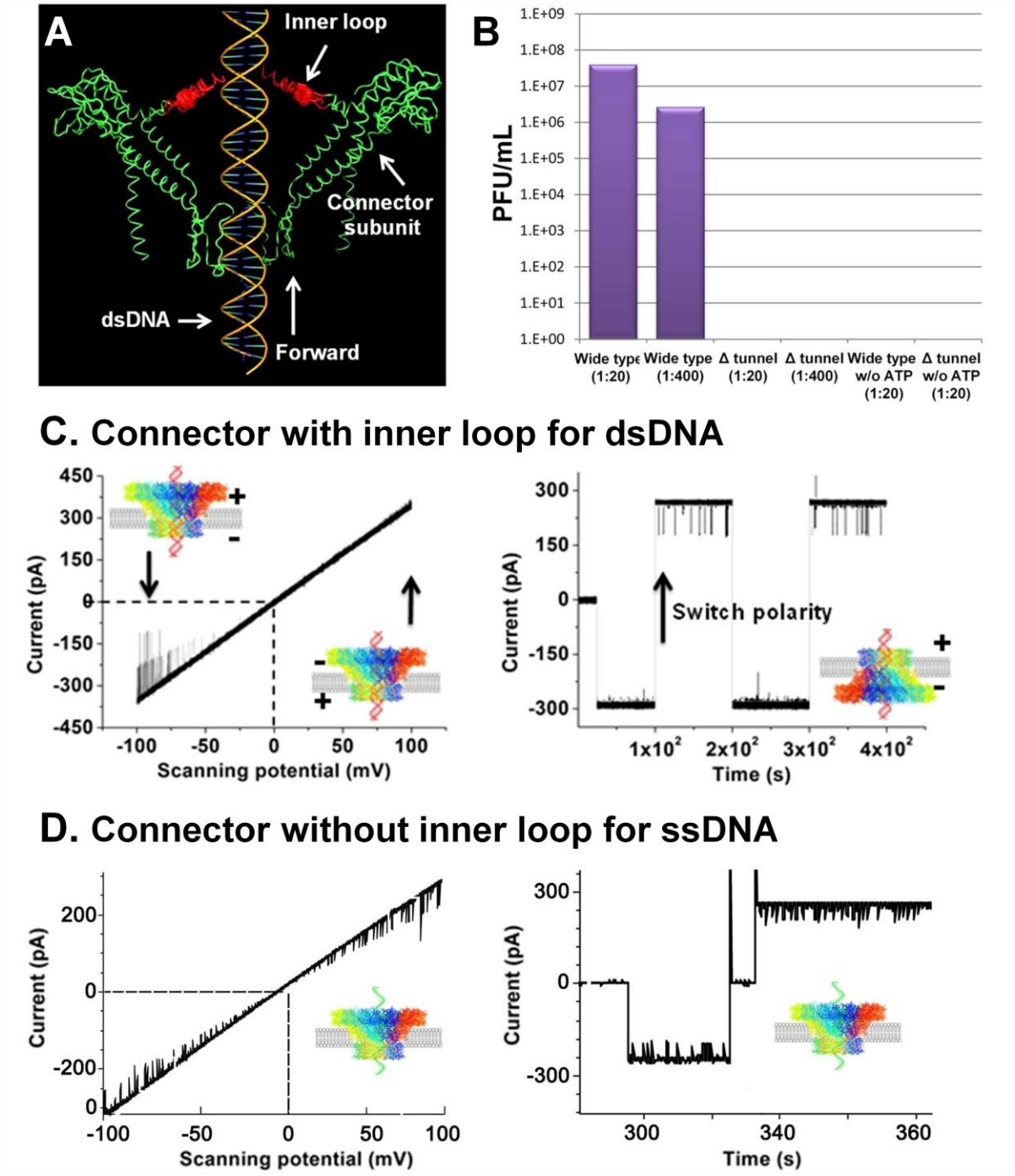

Figure 6. The role of the flexible inner channel loop in DNA one-way traffic. (A) Illustration showing that the flexible loop within the connector channel for controlling DNA in forward moving, but blocks DNA reversal during packaging. **(B)** Two dilutions of wild-type procapsid show high virion assembly activity (~10^7 pfu/ml), while procapsids harboring the connectors with internal loops deletion have very low virion assembly activity. **(C)** Demonstration of one-way traffic of dsDNA through wild-type connectors using a ramping potential from -100mV to +100mV (left), and by switching polarity (right). Under the same condition, ssDNA exhibits two-way traffic **(D)** using a loop deleted connector.

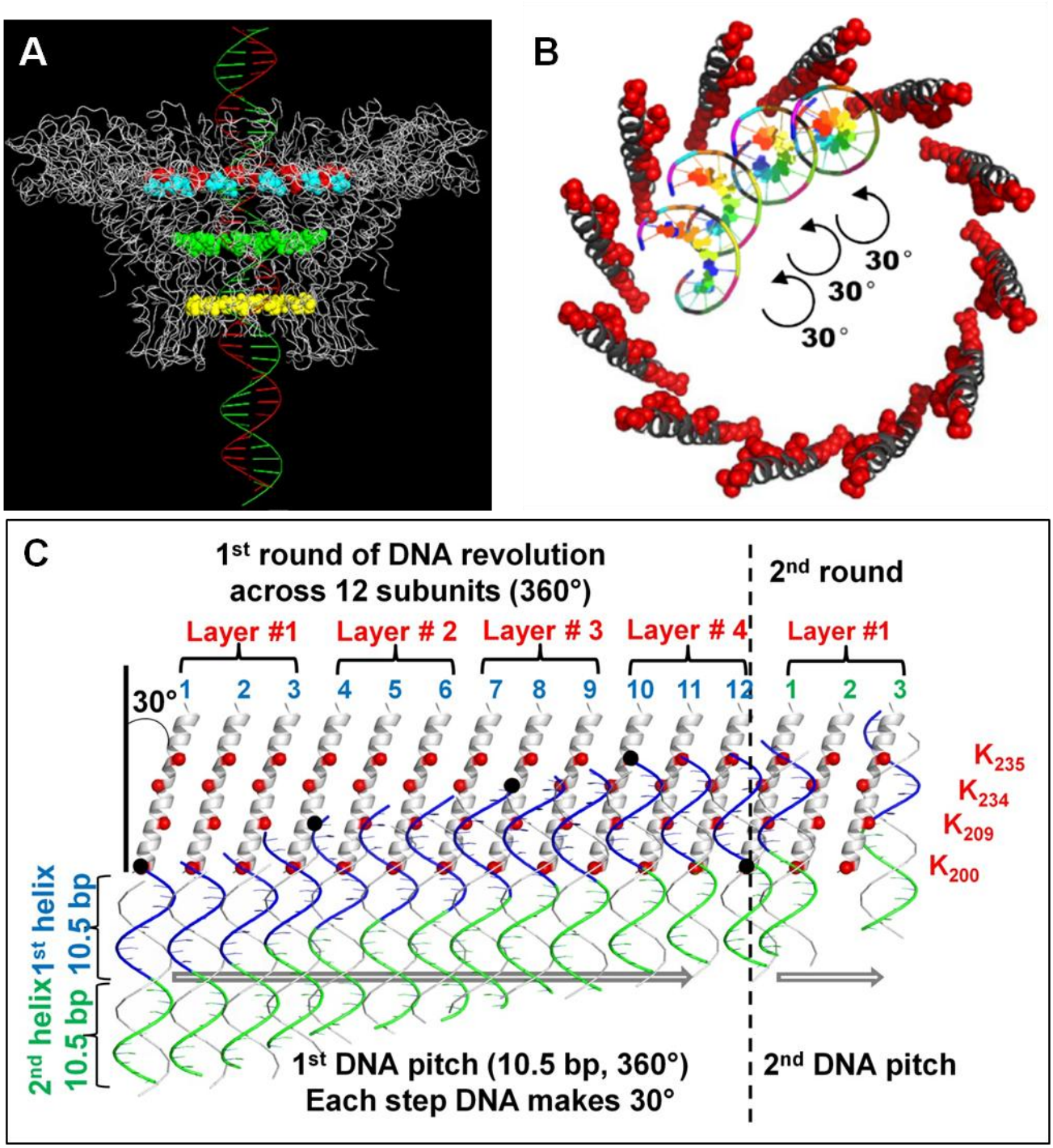

Figure 7. Structure of the phi29 DNA packaging motor showing the four lysine rings scattered inside the inner wall and the DNA revolution inside phi29 connector channel. (A) Side view of the connector, showing K200 (yellow) and K209 (green) lysine rings. The 229 (cyan) with 246 (red) residues show the boundary of the connector inner flexible loop that harbors the other two lysine rings. Due to the flexibility, the crystal structure of the loop is not available; instead the known boundary of the loop was used to estimate the location. Top view **(B)** and side view **(C)** of the detailed schema of DNA revolution through connector is shown in which the negatively-charged phosphate backbone of

dsDNA makes contact with the four lysine layers lending to 4 discrete pauses during packaging of 10.5 bp of genomic dsDNA.

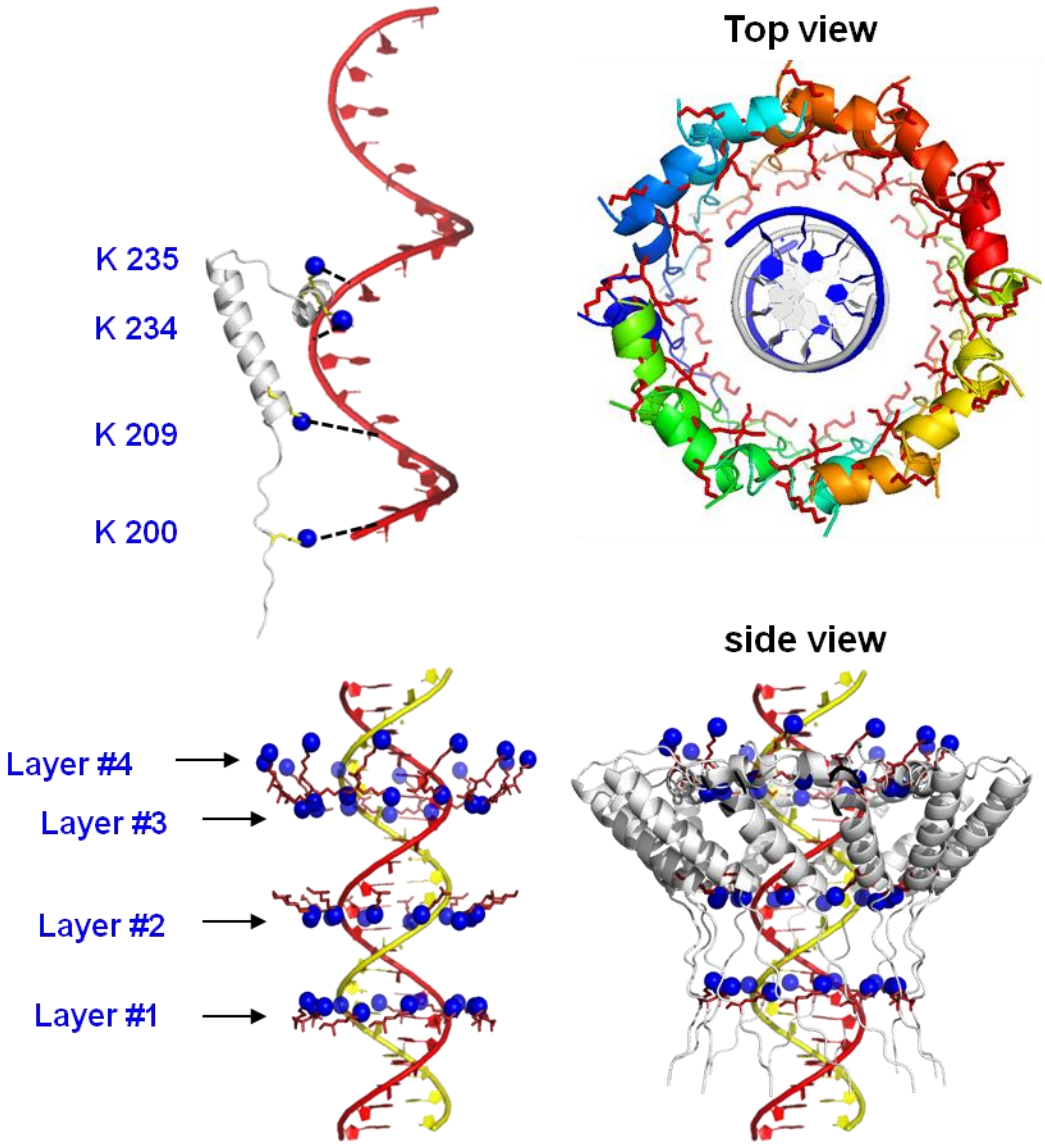

Figure 8. Illustration of the interaction of DNA with connector channel. The size of protein subunits and DNA are according to their 3D structures (connector PDB ID# 1JNB, DNA PDB ID # 3BSE).

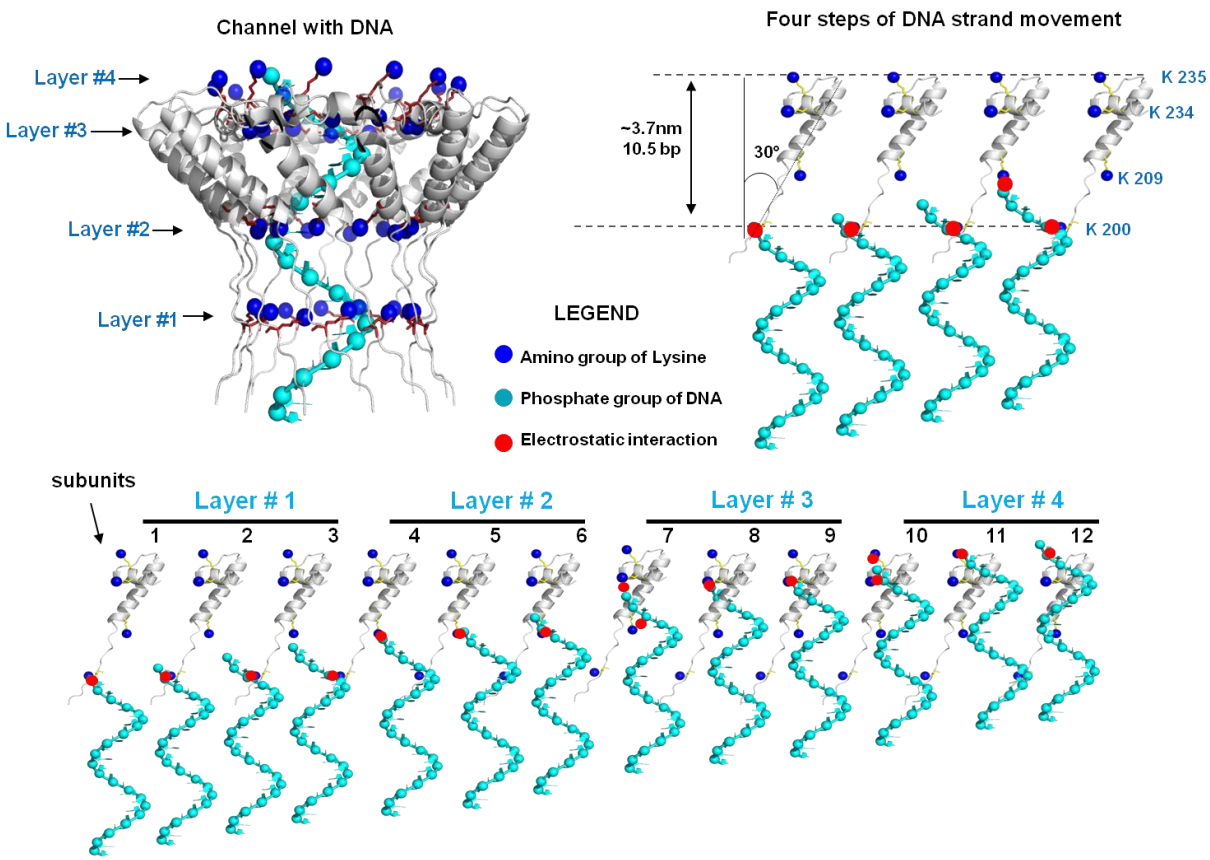

Figure 9. Illustration of the dsDNA revolving through connector channel. Detailed schematic of dsDNA translocation through a channel wall.

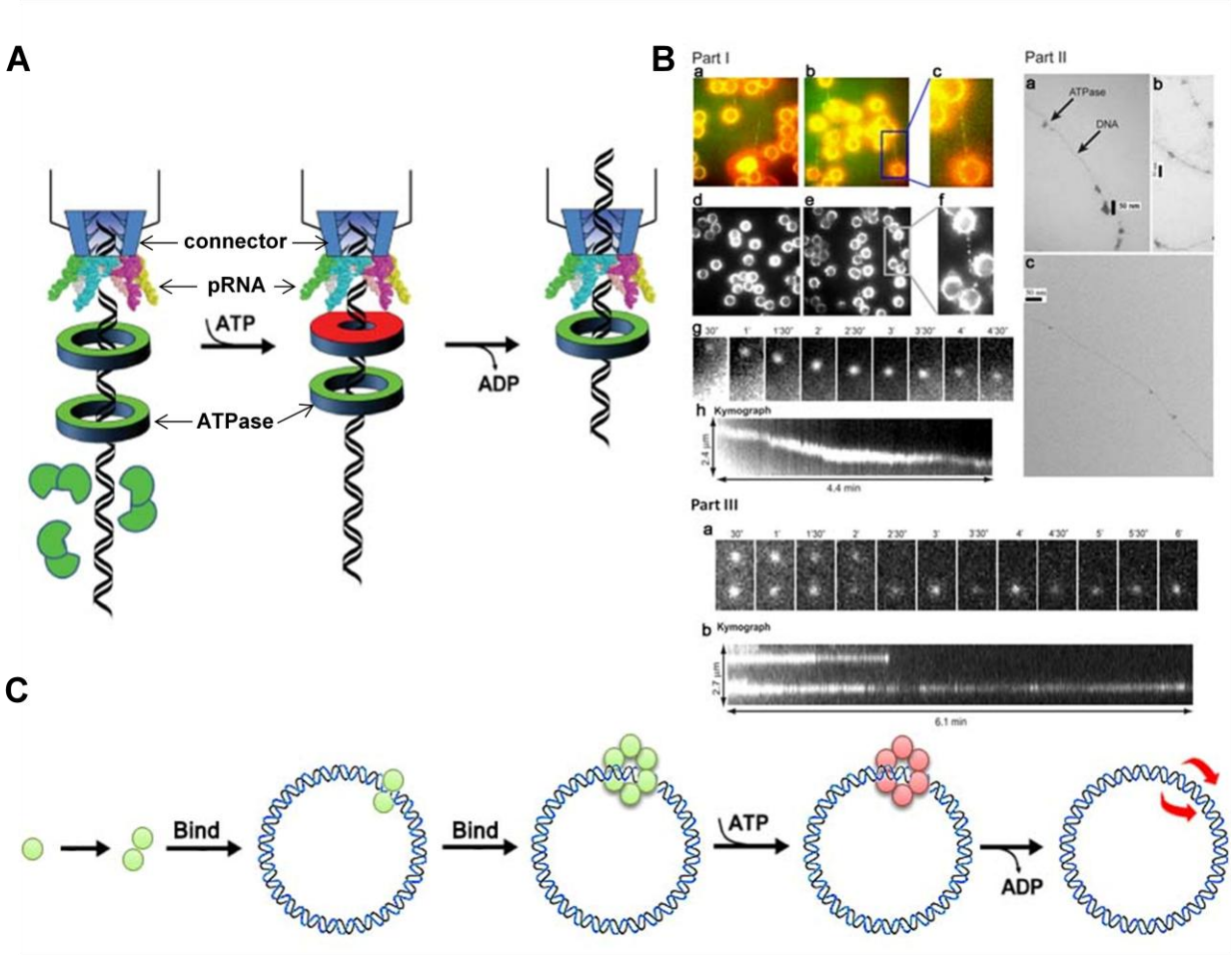

Figure 10. Elucidation showing how does the motor transport closed circular dsDNA without breaking any covalent-bonds or changing the topology of the DNA. (A) Elucidation of sequential action and **"**push through one-way valve mechanism" of phi29 DNA-packaging motor. **(B) Part I.** Direct observation of ATPase complexes queue and move along dsDNA. Cy3 conjugated gp16 were incubated with **(a,b,e)** and without (**d**) phi29 genomic dsDNA tethered between two polylysine beads. The c and f are zoomed-in images of the framed regions of b and e, respectively. The **a-c are** overlapped, pseudocolor images indicating the binding of Cy3-labeled gp16 along the To-Pro-3 stained dsDNA chain (Red: Cy3-gp16; Green: To-Pro-3 DNA). g and h show analysis of the motion of the Cy3-gp16 spot. Kymograph was produced to characterize the ATPase motion. (Use Internet Explorer to view website http://nanobio.uky.edu/movie.html for actual motion videos). **Part II.** Negatively-stained transmission electron microscopy images of ATPase queued along dsDNA. gp16 was bound to non-specific dsDNA in queue. **Part III.** Negative control of recording of two Cy3-gp16/dsDNA complexes showing motionless gp16 spots in a buffer that did not contain ATP. **(C)** Illustration showing the assembly of the motor subunit on circular dsDNA. Subunits gather around the dsDNA chain first and then form a hexamer complex surrounding the DNA.

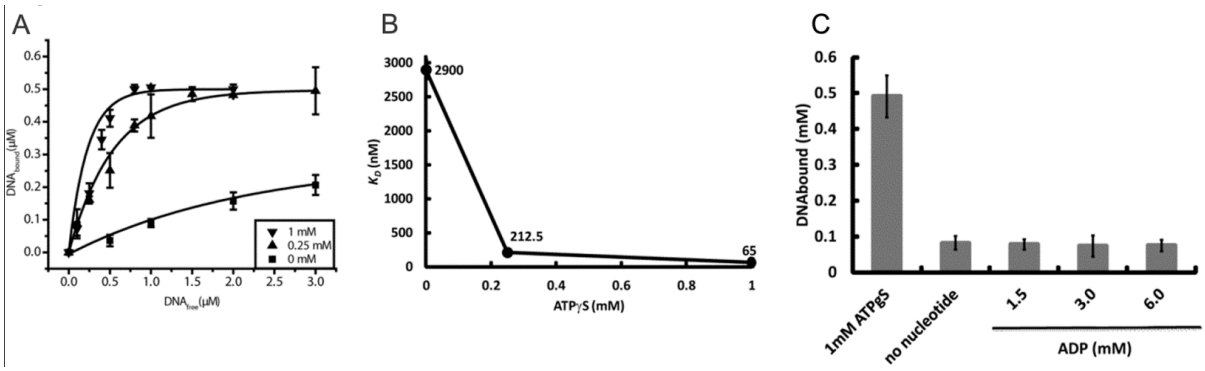

Figure 11. Sequential binding of gp16 with dsDNA substrate involves a γ-s-ATP substep. (A) The Kd for dsDNA in the presence (triangles) and absence (squares) of γ-s-ATP. **(B)** The relative Kd of gp16 decreased 40-fold as the concentration of γ-s-ATP was increased from 0 mM to 1 mM. **(C)** ADP, a derivative of ATP hydrolysis, was unable to promote binding and had the similar effect as that of no nucleotide addition.

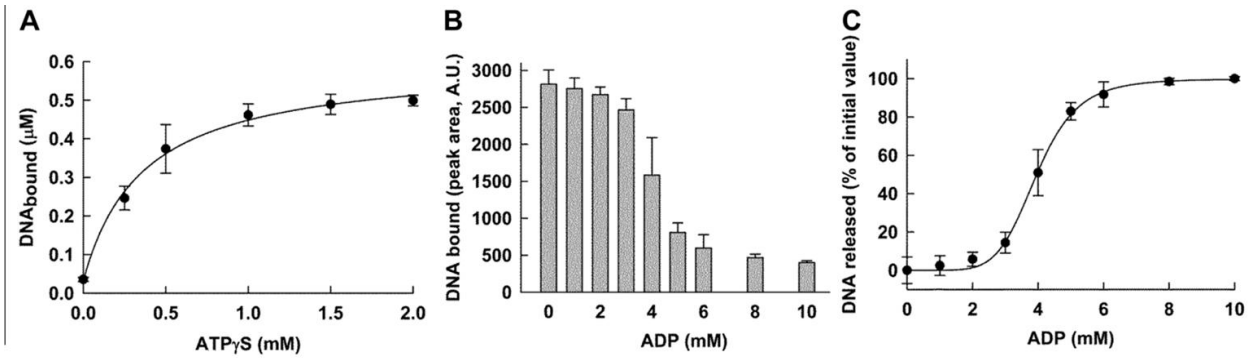

Figure 12. Data demonstrating that only one γ-s-ATP is needed to bind to one subunit of the hexameric gp16 complex and promote a high affinity state for dsDNA. The hyperbolic curve **(A)** suggests a cooperativity factor of 1, indicating that one γ-s-ATP is sufficient to produce the high affinity state of gp16 for DNA. DNA is released from the DNA-gp16-γ-s-ATP complex mediated by ADP **(B)**, forming a sigmoidal curve **(C)** with a cooperativity factor of 6; indicating that all 6 subunits of gp16 are needed to be bound to ADP in order to release DNA from the protein.

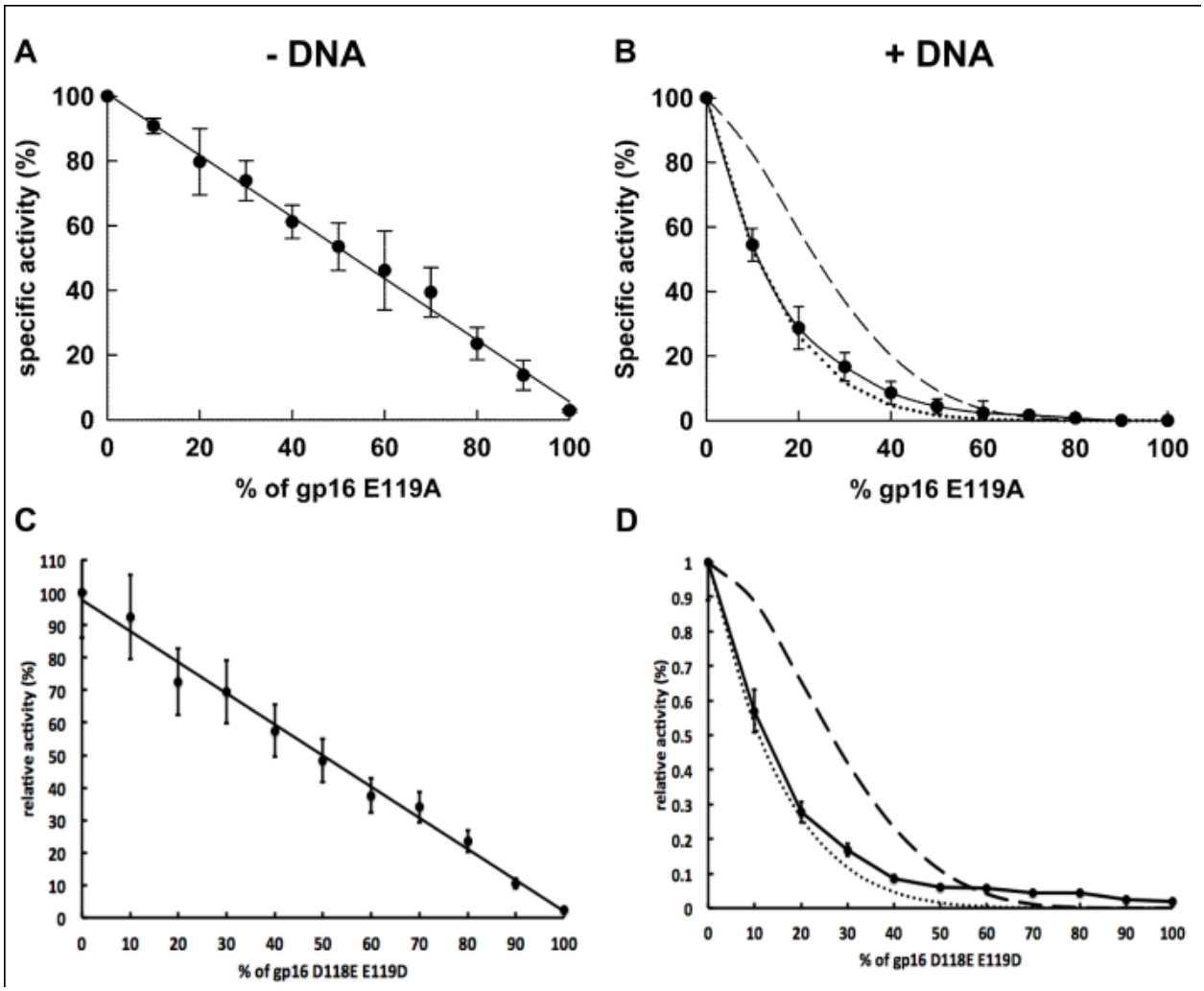

Figure 13. ATPase inhibition assay of Walker B mutants reveal complete negative cooperativity. The inhibition ability of the Walker B mutants E119A and D118E/E119D was assayed by ATPase activity to determine the theoretical model in the absence (left) and presence (right) of dsDNA. In the presence of DNA (right), the experimental data (solid line) overlapped with the theoretical curve indicating that one inactive subunit (dotted line) within the hexamer is able to completely block the activity of the hexameric gp16 and abolish gp16's ability to hydrolyze ATP, demonstrating negative cooperativity. The dashed line is the theoretical curve representing two inactive subunits that are necessary for complete inhibition of the hexamer.

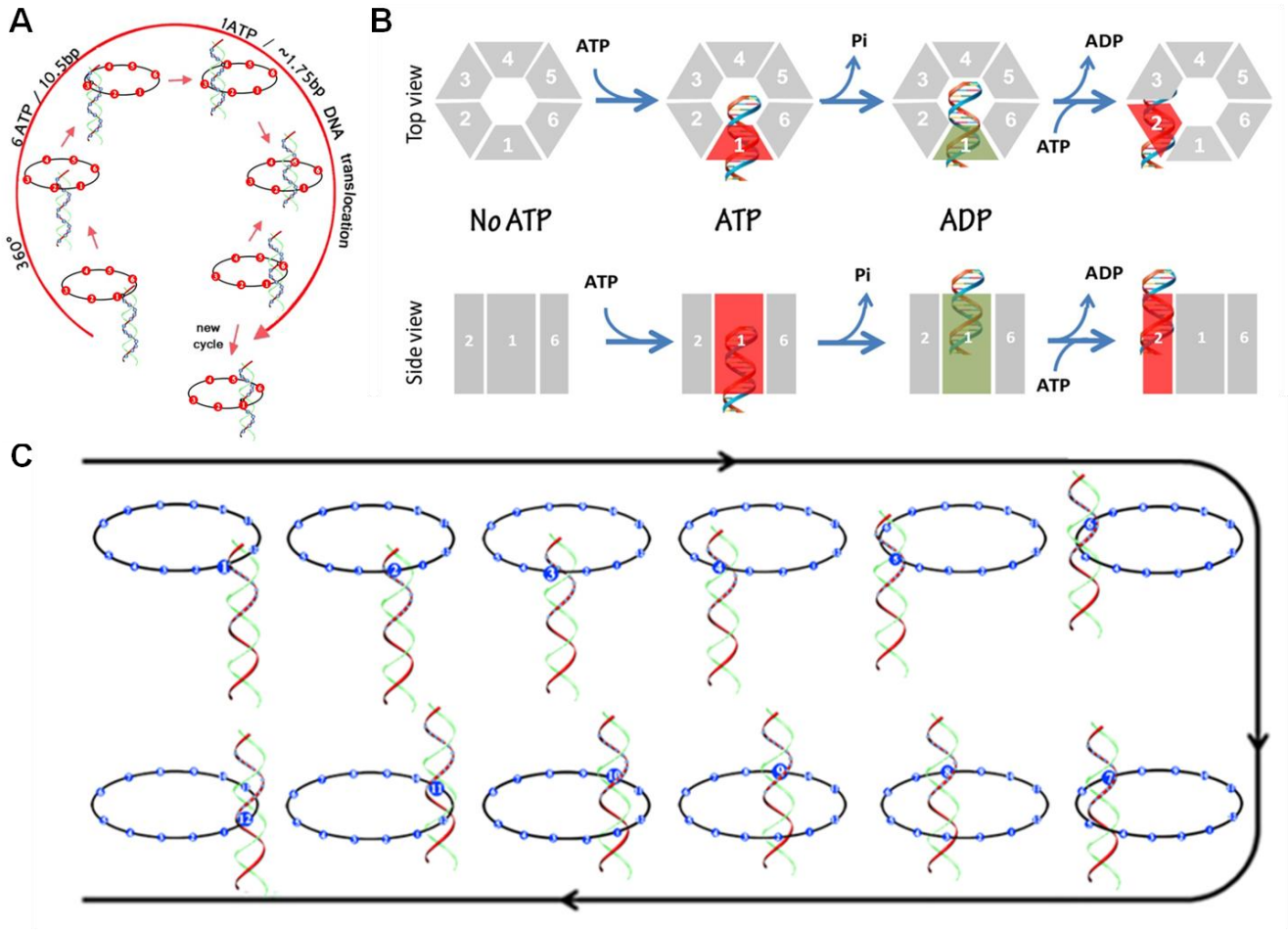

Figure 14. Schematic of gp16 binding to DNA and the mechanism of sequential revolution in translocating genomic DNA. ATP hydrolysis forces gp16 to assume a new conformation with a lower affinity for dsDNA, thus pushing dsDNA away from the subunit and transferring it to an adjacent subunit. **(A,B)** The binding of gp16 to the same phosphate backbone chain, but at a location 60° different from last subunit, urges dsDNA to move forward 1.75 base pairs. Since the dsDNA chain is transferred from one point on the phosphate backbone to another point, neither the rotation of the hexameric ring nor the dsDNA is required. One ATP is hydrolyzed in each transitional step, and six ATPs are consumed in one cycle to translocate dsDNA 360° (10.5 base pairs). Please see attached website using Internet Explorer http://nanobio.uky.edu/movie.html for animations. **(C)** The revolution of dsDNA along the 12 subunits of the connector channel in a planar format.

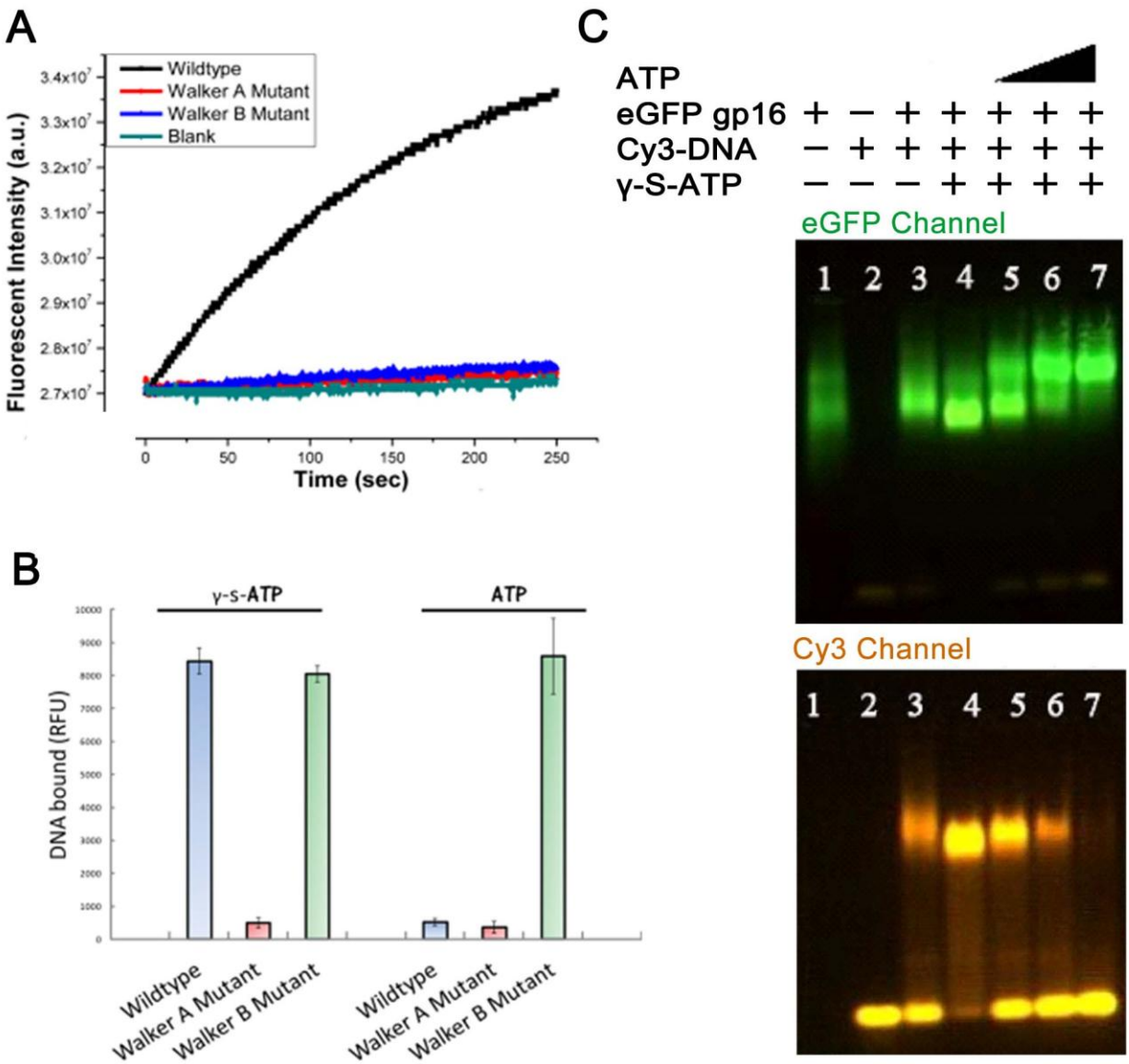

Figure 15. Assay of ATPase gp16 for ATPase activity and dsDNA binding. **(A)** Both Walker motif mutants are unable to hydrolyze ATP, but the **(B)** Walker B mutant can still bind dsDNA in the presence of an ATP analog. ATP did not release dsDNA from the gp16/dsDNA complex when Walker B was mutated (B, green). **(C)** Two conformational states of gp16 (DNA-bound or DNA-unbound) are shown in the EMSA.

Reference List

1. Aathavan, K., Politzer, A. T., Kaplan, A., Moffitt, J. R., Chemla, Y. R., Grimes, S., Jardine, P. J., Anderson, D. L., Bustamante, C., 2009. Substrate interactions and promiscuity in a viral DNA packaging motor. Nature 461, 669-673.
2. Acharya, S., Foster, P. L., Brooks, P., Fishel, R., 2003. The coordinated functions of the E. coli MutS and MutL proteins in mismatch repair. Mol.Cell 12, 233-246.
3. Aker, J., Hesselink, R., Engel, R., Karlova, R., Borst, J. W., Visser, A. J. W. G., de Vries, S. C., 2007. *In vivo* hexamerization and characterization of the Arabidopsis AAA ATPase CDC48A complex using forster resonance energy transfer-fluorescence lifetime imaging microscopy and fluorescence correlation spectroscopy. Plant Physiology 145, 339-350.
4. Amitani, I., Baskin, R. J., Kowalczykowski, S. C., 2006. Visualization of Rad54, a chromatin remodeling protein, translocating on single DNA molecules. Mol.Cell 23, 143-148.
5. Ammelburg, M., Frickey, T., Lupas, A. N., 2006. Classification of AAA+ proteins. Journal of Structural Biology 156, 2-11.
6. Badasso, M. O., Leiman, P. G., Tao, Y., He, Y., Ohlendorf, D. H., Rossmann, M. G., Anderson, D., 2000. Purification, crystallization and initial X-ray analysis of the head- tail connector of bacteriophage phi29. Acta Crystallogr D Biol Crystallogr 56 (Pt 9), 1187-1190.
7. Bath, J., Wu, L. J., Errington, J., Wang, J. C., 2000. Role of Bacillus subtilis SpoIIIE in DNA transport across the mother cell-prespore division septum. Science 290, 995-997.
8. Black, L. W., 1989. DNA Packaging in dsDNA bacteriophages. Annual Review of Microbiology 43, 267-292.
9. Bourassa, N., Major, F., 2002. Implication of the prohead RNA in phage phi29 DNA packaging. Biochimie 84, 945-951.
10. Casjens, S. R., 2011. The DNA-packaging nanomotor of tailed bacteriophages. Nat Rev.Microbiol. 9, 647-657.
11. Chad Schwartz, Gian Marco De Donatis, Huaming Fang, Peixuan Guo, 2013. Mechanism of action by the hexameric phi29 DNA-packaging motor. Virology In submission.
12. Chang, J. R., Andrews, B. T., Catalano, C. E., 2012. Energy-independent helicase activity of a viral genome packaging motor. Biochemistry 51, 391-400.
13. Chemla, Y. R., Aathavan, K., Michaelis, J., Grimes, S., Jardine, P. J., Anderson, D. L., Bustamante, C., 2005. Mechanism of force generation of a viral DNA packaging motor. Cell. 122, 683-692.
14. Chen, C., Guo, P., 1997b. Sequential action of six virus-encoded DNA-packaging RNAs during phage phi29 genomic DNA translocation. Journal of Virology 71, 3864-3871.
15. Chen, C., Guo, P., 1997a. Magnesium-induced conformational change of packaging RNA for procapsid recognition and binding during phage phi29 DNA encapsidation. Journal of Virology 71, 495-500.
16. Chen, C., Trottier, M., Guo, P., 1997. New approaches to stoichiometry determination and mechanism investigation on RNA involved in intermediate reactions. Nucleic Acids Symposium Series 36, 190-193.
17. Chen, Y. J., Yu, X., Egelman, E. H., 2002. The hexameric ring structure of the Escherichia coli RuvB branch migration protein. J.Mol.Biol. 319, 587-591.

18. Chistol, G., Liu, S., Hetherington, C. L., Moffitt, J. R., Grimes, S., Jardine, P. J., Bustamante, C., 2012b. High Degree of Coordination and Division of Labor among Subunits in a Homomeric Ring ATPase. Cell 151, 1017-1028.
19. Chistol, G., Liu, S., Hetherington, C. L., Moffitt, J. R., Grimes, S., Jardine, P. J., Bustamante, C., 2012a. High Degree of Coordination and Division of Labor among Subunits in a Homomeric Ring ATPase. Cell 151, 1017-1028.
20. Demarre, G., Galli, E., Barre, F. X., 2013. The FtsK Family of DNA Pumps. Adv.Exp.Med.Biol 767, 245-262.
21. Fang, H., Jing, P., Haque, F., Guo, P., 2012. Role of channel Lysines and "Push Through a One-way Valve" Mechanism of Viral DNA packaging Motor. Biophysical Journal 102, 127-135.
22. Feiss, M., Rao, V. B., 2012. The Bacteriophage DNA Packaging Machine Viral Molecular Machines. In: M. G. Rossmann, V. B. Rao (Eds.), Springer US, pp. 489-509.
23. Fujisawa, H., Shibata, H., Kato, H., 1991. Analysis of interactions among factors involved in the bacteriophage T3 DNA packaging reaction in a defined *in vitro* system. Virology 185, 788-794.
24. Geng, J., Fang, H., Haque, F., Zhang, L., Guo, P., 2011. Three reversible and controllable discrete steps of channel gating of a viral DNA packaging motor. Biomaterials 32, 8234-8242.
25. Geng, J., Fang, H., Wang, S., Guo P, 2013. Channel Size Conversion of Phi29 DNA-Packaging Nanomotor for Discrimination of Single- and Double-Stranded DNA and RNA. ACS Nano In submission.
26. Gomis-Ruth, F. X., Moncalian, G., Perez-Luque, R., Gonzalez, A., Cabezon, E., de la, C. F., Coll, M., 2001. The bacterial conjugation protein TrwB resembles ring helicases and F1-ATPase. Nature 409, 637-641.
27. Gradia, S., Acharya, S., Fishel, R., 1997. The human mismatch recognition complex hMSH2-hMSH6 functions as a novel molecular switch. Cell 91, 995-1005.
28. Gradia, S., Subramanian, D., Wilson, T., Acharya, S., Makhov, A., Griffith, J., Fishel, R., 1999. hMSH2-hMSH6 forms a hydrolysis-independent sliding clamp on mismatched DNA. Mol.Cell 3, 255-261.
29. Grigoriev, D. N., Moll, W., Hall, J., Guo, P., 2004. Bionanomotor. In: H. S. Nalwa (Ed.), Encyclopedia of Nanoscience and Nanotechnology. American Scientific Publishers., pp. 361-374.
30. Grimes, S., Anderson, D., 1990. RNA Dependence of the Bateriophage phi29 DNA Packaging ATPase. J.Mol.Biol. 215, 559-566.
31. Grimes, S., Ma, S., Gao, J., Atz, R., Jardine, P. J., 2011. Role of phi29 connector channel loops in late-stage DNA packaging. J.Mol.Biol. 410, 50-59.
32. Guasch, A., Pous, J., Ibarra, B., Gomis-Ruth, F. X., Valpuesta, J. M., Sousa, N., Carrascosa, J. L., Coll, M., 2002. Detailed architecture of a DNA translocating machine: the high- resolution structure of the bacteriophage phi29 connector particle. J.Mol.Biol. 315, 663-676.
33. Guenther, B., Onrust, R., Sali, A., O'Donnell, M., Kuriyan, J., 1997. Crystal structure of the delta' subunit of the clamp-loader complex of E. coli DNA polymerase III. Cell 91, 335-345.
34. Guo, P., Erickson, S., Anderson, D., 1987. A small viral RNA is required for *in vitro* packaging of bacteriophage phi29 DNA. Science 236, 690-694.
35. Guo, P., Grimes, S., Anderson, D., 1986. A defined system for *in vitro* packaging of DNA-gp3 of the *Bacillus subtilis* bacteriophage phi29. Proc.Natl.Acad.Sci.USA 83, 3505-3509.
36. Guo, P., Peterson, C., Anderson, D., 1987a. Initiation events in *in vitro* packaging of bacteriophage ϕ29 DNA-gp3. Journal of Molecular Biology 197, 219-228.

37. Guo, P., Peterson, C., Anderson, D., 1987b. Prohead and DNA-gp3-dependent ATPase activity of the DNA packaging protein gp16 of bacteriophage ϕ29. Journal of Molecular Biology 197, 229-236.
38. Guo, P., Zhang, C., Chen, C., Trottier, M., Garver, K., 1998. Inter-RNA interaction of phage phi29 pRNA to form a hexameric complex for viral DNA transportation. Molecular Cell 2, 149-155.
39. Guo, P. X., Lee, T. J., 2007. Viral nanomotors for packaging of dsDNA and dsRNA. Molecular Microbiology 64, 886-903.
40. Hendrix, R. W., 1998. Bacteriophage DNA packaging: RNA gears in a DNA transport machine (Minireview). Cell 94, 147-150.
41. Hendrix, R. W., 1978. Symmetry mismatch and DNA packaging in large bacteriophages. Proc.Natl.Acad.Sci.USA 75, 4779-4783.
42. Huang, L. P., Guo, P., 2003a. Use of acetone to attain highly active and soluble DNA packaging protein gp16 of phi29 for ATPase assay. Virology 312(2), 449-457.
43. Huang, L. P., Guo, P., 2003b. Use of PEG to acquire highly soluble DNA-packaging enzyme gp16 of bacterial virus phi29 for stoichiometry quantification. J Virol Methods 109, 235-244.
44. Hugel, T., Michaelis, J., Hetherington, C. L., Jardine, P. J., Grimes, S., Walter, J. M., Faik, W., Anderson, D. L., Bustamante, C., 2007. Experimental test of connector rotation during DNA packaging into bacteriophage phi29 capsids. Plos Biology 5, 558-567.
45. Hwang, Y., Catalano, C. E., Feiss, M., 1996. Kinetic and mutational dissection of the two ATPase activities of terminase, the DNA packaging enzyme of bacteriophage lambda. Biochemistry 35, 2796-2803.
46. Ibarra B, Caston J.R., Llorca O., Valle M, Valpuesta J.M., Carrascosa J.L., 2000. Topology of the components of the DNA packaging machinery in the phage phi29 prohead. J.Mol.Biol. 298, 807-815.
47. Ibarra, B., Valpuesta, J. M., Carrascosa, J. L., 2001. Purification and functional characterization of p16, the ATPase of the bacteriophage phi29 packaging machinary. Nucleic Acids Research 29(21), 4264-4273.
48. Isidro, A., Henriques, A. O., Tavares, P., 2004. The portal protein plays essential roles at different steps of the SPP1 DNA packaging process. Virology. 322, 253-263.
49. Iyer, L. M., Makarova, K. S., Koonin, E. V., Aravind, L., 2004. Comparative genomics of the FtsK-HerA superfamily of pumping ATPases: implications for the origins of chromosome segregation, cell division and viral capsid packaging. Nucleic Acids Research 32, 5260-5279.
50. Jimenez, J., Santisteban, A., Carazo, J. M., Carrascosa, J. L., 1986. Computer graphic display method for visualizing three-dimensional biological structures. Science 232, 1113-1115.
51. Jing, P., Haque, F., Shu, D., Montemagno, C., Guo, P., 2010. One-Way Traffic of a Viral Motor Channel for Double-Stranded DNA Translocation. Nano Lett. 10 (9), 3620-3627.
52. Kinosita, K., Jr., Yasuda, R., Noji, H., Adachi, K., 2000. A rotary molecular motor that can work at near 100% efficiency. Philos.Trans.R.Soc.Lond B Biol.Sci. 355, 473-489.
53. Lee, C. S., Guo, P., 1994. A highly sensitive system for the *in vitro* assembly of bacteriophage phi29 of *Bacillus subtilis*. Virology 202, 1039-1042.
54. Lee, C. S., Guo, P., 1995. *In vitro* assembly of infectious virions of ds-DNA phage ϕ29 from cloned gene products and synthetic nucleic acids. Journal of Virology 69, 5018-5023.
55. Lee, T. J., Guo, P., 2006. Interaction of gp16 with pRNA and DNA for genome packaging by the motor of bacterial virus phi29. J.Mol Biol. 356, 589-599.
56. Lee, T. J., Zhang, H., Liang, D., Guo, P., 2008. Strand and nucleotide-dependent ATPase activity of gp16 of bacterial virus phi29 DNA packaging motor. Virology 380, 69-74.

57. Maluf, N. K., Gaussier, H., Bogner, E., Feiss, M., Catalano, C. E., 2006. Assembly of Bacteriophage Lambda Terminase into a Viral DNA Maturation and Packaging Machine. Biochemistry. 45, 15259-15268.
58. Martin, A., Baker, T. A., Sauer, R. T., 2005. Rebuilt AAA + motors reveal operating principles for ATP-fuelled machines. Nature 437, 1115-1120.
59. Massey, T. H., Mercogliano, C. P., Yates, J., Sherratt, D. J., Lowe, J., 2006. Double-stranded DNA translocation: structure and mechanism of hexameric FtsK. Mol.Cell 23, 457-469.
60. McNally, R., Bowman, G. D., Goedken, E. R., O'Donnell, M., Kuriyan, J., 2010. Analysis of the role of PCNA-DNA contacts during clamp loading. BMC.Struct.Biol. 10, 3.
61. Mi, J., Liu, Y., Rabbani, Z. N., Yang, Z., Urban, J. H., SULLENGER, B. A., Clary, B. M., 2010. In vivo selection of tumor-targeting RNA motifs. Nature Chemical Biology 6, 22-24.
62. Moffitt, J. R., Chemla, Y. R., Aathavan, K., Grimes, S., Jardine, P. J., Anderson, D. L., Bustamante, C., 2009. Intersubunit coordination in a homomeric ring ATPase. Nature 457, 446-450.
63. Moll, D., Guo, P., 2007. Grouping of Ferritin and Gold Nanoparticles Conjugated to pRNA of the Phage phi29 DNA-packaging motor. J Nanosci and Nanotech (JNN) 7, 3257-3267.
64. Moll, W.-D., Guo, P., 2005. Translocation of Nicked but not Gapped DNA by the Packaging Motor of Bacteriophage phi29. Journal of Molecular Biology 351, 100-107.
65. Morais, M. C., Koti, J. S., Bowman, V. D., Reyes-Aldrete, E., Anderson D, Rossman, M. G., 2008. Defining molecular and domain boundaries in the bacteriophage phi29 DNA packaging motor. Structure 16, 1267-1274.
66. Morais, M. C., Tao Y, Olsen, N. H., Grimes, S., Jardine, P. J., Anderson, D., Baker TS, Rossmann, M. G., 2001. Cryoelectron-Microscopy Image Reconstruction of Symmetry Mismatches in Bacteriophage phi29. Journal of Structural Biology 135, 38-46.
67. Mueller-Cajar, O., Stotz, M., Wendler, P., Hartl, F. U., Bracher, A., Hayer-Hartl, M., 2011. Structure and function of the AAA+ protein CbbX, a red-type Rubisco activase. Nature 479, 194-199.
68. Oram, M., Sabanayagam, C., Black, L. W., 2008. Modulation of the Packaging Reaction of Bacteriophage T4 Terminase by DNA Structure. Journal of Molecular Biology 381, 61-72.
69. Rao, V. B., Feiss, M., 2008. The Bacteriophage DNA Packaging Motor. Annu.Rev.Genet. 42, 647-681.
70. Ray, K., Ma, J., Oram, M., Lakowicz, J. R., Black, L. W., 2010. Single-molecule and FRET fluorescence correlation spectroscopy analyses of phage DNA packaging: colocalization of packaged phage T4 DNA ends within the capsid. J.Mol.Biol. 395, 1102-1113.
71. Ray, K., Sabanayagam, C. R., Lakowicz, J. R., Black, L. W., 2010. DNA crunching by a viral packaging motor: Compression of a procapsid-portal stalled Y-DNA substrate. Virology 398, 224-232.
72. Roy, A., Bhardwaj, A., Cingolani, G., 2011a. Crystallization of the nonameric small terminase subunit of bacteriophage P22. Acta Crystallographica Section F-Structural Biology and Crystallization Communications 67, 104-110.
73. Roy, A., Bhardwaj, A., Cingolani, G., 2011b. Crystallization of the nonameric small terminase subunit of bacteriophage P22. Acta Crystallographica Section F-Structural Biology and Crystallization Communications 67, 104-110.
74. Sabanayagam, C. R., Oram, M., Lakowicz, J. R., Black, L. W., 2007. Viral DNA packaging studied by fluorescence correlation spectroscopy. Biophys.J 93, L17-L19.
75. Schwartz, C., De Donatis, G. M., Fang, H., Guo, P., 2013b. Mechanism of mighty force generation of the hexameric phi29 DNA-packaging motor. Virology.

76. Schwartz, C., De Donatis, G. M., Fang, H., Guo, P., 2013a. Mechanism of mighty force generation of the hexameric phi29 DNA-packaging motor. Virology.
77. Schwartz, C., Fang, H., Huang, L., Guo, P., 2012. Sequential action of ATPase, ATP, ADP, Pi and dsDNA in procapsid-free system to enlighten mechanism in viral dsDNA packaging. Nucleic Acids Research 40, 2577-2586.
78. Schwartz, C., Zhang, H., Fang, H., De Donatis, G. M., Guo, P., 2013a. Revolution rather than rotation of AAA+ hexameric phi29 nanomotor for viral dsDNA packaging without coiling. Virology.
79. Schwartz, C., Zhang, H., Fang, H., De Donatis, G. M., Guo, P., 2013b. Revolution rather than rotation of AAA+ hexameric phi29 nanomotor for viral dsDNA packaging without coiling. Virology.
80. Serwer, P., 2003. Models of bacteriophage DNA packaging motors. J Struct.Biol 141, 179-188.
81. Serwer, P., 2010. A Hypothesis for Bacteriophage DNA Packaging Motors. Viruses-Basel 2, 1821-1843.
82. Shu, D., Zhang, H., Jin, J., Guo, P., 2007. Counting of six pRNAs of phi29 DNA-packaging motor with customized single molecule dual-view system. EMBO Journal **26**, 527-537.
83. Sim, J., Ozgur, S., Lin, B. Y., Yu, J. H., Broker, T. R., Chow, L. T., Griffith, J., 2008. Remodeling of the Human Papillomavirus Type 11 Replication Origin into Discrete Nucleoprotein Particles and Looped Structures by the E2 Protein. Journal of Molecular Biology 375, 1165-1177.
84. Simpson, A. A., Leiman, P. G., Tao, Y., He, Y., Badasso, M. O., Jardine, P. J., Anderson, D. L., Rossman, M. G., 2001. Structure determination of the head-tail connector of bacteriophage phi29. Acta Cryst D57, 1260-1269.
85. Simpson, A. A., Tao, Y., Leiman, P. G., Badasso, M. O., He, Y., Jardine, P. J., Olson, N. H., Morais, M. C., Grimes, S., Anderson, D. L., Baker, T. S., Rossmann, M. G., 2000. Structure of the bacteriophage phi29 DNA packaging motor. Nature 408, 745-750.
86. Skordalakes, E., Berger, J. M., 2006. Structural Insights into RNA-Dependent Ring Closure and ATPase Activation by the Rho Termination Factor. Cell 127, 553-564.
87. Smith, D. E., Tans, S. J., Smith, S. B., Grimes, S., Anderson, D. L., Bustamante, C., 2001. The bacteriophage phi29 portal motor can package DNA against a large internal force. Nature 413, 748-752.
88. Snider, J., Houry, W. A., 2008. AAA+ proteins: diversity in function, similarity in structure. Biochemical Society Transactions 36, 72-77.
89. Snider, J., Thibault, G., Houry, W. A., 2008. The AAA+ superfamily of functionally diverse proteins. Genome Biol 9, 216.
90. Story, R. M., Steitz, T. A., 1992. Structure of the rec-A protein-ADP Complex. Nature 355.
91. Trottier, M., Guo, P., 1997. Approaches to determine stoichiometry of viral assembly components. Journal of Virology 71, 487-494.
92. Vale, R., 1993. Motor proteins. In: T. Kreis, R. Vale (Eds.), Guidebook to the Cytoskeletal and Motor Proteins. Oxford University Press, pp. 175-211.
93. Wang, F., Mei, Z., Qi, Y., Yan, C., Hu, Q., Wang, J., Shi, Y., 2011. Structure and mechanism of the hexameric MecA-ClpC molecular machine. Nature 471, 331-335.
94. Wendell, D., Jing, P., Geng, J., Subramaniam, V., Lee, T. J., Montemagno, C., Guo, P., 2009. Translocation of double-stranded DNA through membrane-adapted phi29 motor protein nanopores. Nature Nanotechnology 4, 765-772.
95. Willows, R. D., Hansson, A., Birch, D., Al-Karadaghi, S., Hansson, M., 2004. EM single particle analysis of the ATP-dependent BchI complex of magnesium chelatase: an AAA(+) hexamer. Journal of Structural Biology 146, 227-233.

96. Xiao, F., Zhang, H., Guo, P., 2008. Novel mechanism of hexamer ring assembly in protein/RNA interactions revealed by single molecule imaging. Nucleic Acids Res 36 (20), 6620-6632.
97. Xiao, F., Demeler, B., Guo, P., 2010. Assembly Mechanism of the Sixty-Subunit Nanoparticles via Interaction of RNA with the Reengineered Protein Connector of phi29 DNA-Packaging Motor. ACS Nano. 4, 3293-3301.
98. Yu, J., Moffitt, J., Hetherington, C. L., Bustamante, C., Oster, G., 2010. Mechanochemistry of a viral DNA packaging motor. J.Mol.Biol. 400, 186-203.
99. Zhang, F., Lemieux, S., Wu, X., St.-Arnaud, S., McMurray, C. T., Major, F., Anderson, D., 1998. Function of hexameric RNA in packaging of bacteriophage phi29 DNA in vitro. Molecular Cell 2, 141-147.
100. Zhang, H., Schwartz, C., De Donatis, G. M., Guo, P., 2012. Hexameric viral DNA packaging motor using a "Push through a one-way valve" mechanism. Adv.Virus Res 83, 415-465.
101. Zhang, H., Endrizzi, J. A., Shu, Y., Haque, F., Guo, P., Chi, Y. I., 2012. The 3WJ core crystal structure reveals divalent ion-promoted thermostability and functional assembly of the phi29 hexameric motor pRNA. RNA Submitted.
102. Zhang, X., Wigley, D. B., 2008. The 'glutamate switch' provides a link between ATPase activity and ligand binding in AAA+ proteins. Nat.Struct.Mol.Biol. 15, 1223-1227.
103. Zhao, Z., Khisamutdinov, E., Schwartz, C., Guo, P., 2013b. Mechanism of one-way traffic of the hexameric DNA Translocation motor by means of anti-parallel helixes and four lysine layers. ACS Nano.
104. Zhao, Z., Khisamutdinov, E., Schwartz, C., Guo, P., 2013a. Mechanism of one-way traffic of the hexameric DNA Translocation motor by means of anti-parallel helixes and four lysine layers. ACS Nano.
105. Ziegelin, G. +., Niedenzu, T., Lurz, R., Saenger, W., Lanka, E., 2003. Hexameric RSF1010 helicase RepA: the structural and functional importance of single amino acid residues. Nucleic Acids Research 31, 5917-5929.